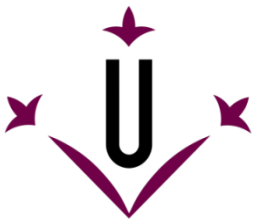

Predicting the spatial and temporal dynamics of species interactions in *Fagus sylvatica* and *Pinus sylvestris* forests across Europe

D. I. Forrester[1,2*], Ch. Ammer[3], P. J. Annighöfer[3], A. Avdagic[4], I. Barbeito[5], K. Bielak[6], G. Brazaitis[7], L. Coll[8], M. del Río[9,10], L. Drössler[11], M. Heym[12], V. Hurt[13], M. Löf[11], B. Matović[14], F. Meloni[15], J. den Ouden[16], M. Pach[17], M. G. Pereira[18], Q. Ponette[19], H. Pretzsch[12] J. Skrzyszewski[17], D. Stojanović[14], M. Svoboda[20], R. Ruiz-Peinado[9,10], G. Vacchiano[15,21], K. Verheyen[22], T. Zlatanov[23], A. Bravo-Oviedo[9,10]

[1]Swiss Federal Institute for Forest, Snow and Landscape Research WSL, Birmensdorf, Switzerland
[2]Chair of Silviculture, Albert-Ludwigs-Universität Freiburg, Germany
[3]Chair of Silviculture and Forest Ecology of the temperate Zones, Georg-August-Universität Göttingen, Germany
[4]Department of Forest management and Urban greenery, Faculty of Forestry, University Sarajevo, Bosnia-Herzegovina
[5]Laboratoire d'Etude des Ressources Forêt Bois (LERFoB), INRA centre of Nancy, Champenoux, France
[6]Department of Silviculture, Warsaw University of Life Sciences, Poland
[7]Institute of Forest Biology and Silviculture, Aleksandras, Stulginskis University, Kaunas, Lithuania
[8]Department of Agriculture and Forest Engineering - Forest Sciences Centre of Catalonia (CTFC), University of Lleida, Spain
[9]Department of Silviculture and Forest Management, INIA, Forest Research Centre INIA-CIFOR Forest Research Centre, Crta. La Coruña km 7,5 28040 Madrid. Spain.
[10]Sustainable Forest Management Research Institute University of Valladolid & INIA
[11]Southern Swedish Forest Research Centre, Swedish University of Agricultural Sciences, Alnarp, Sweden
[12]Chair for Forest Growth and Yield Science, Technische Universität München, Germany
[13]Department of Silviculture, Mendel University, Brno, Czech Republic
[14]Institute of Lowland Forestry and Environment, University of Novi Sad, Novi Sad, Serbia
[15]Department of Agricultural, Forest and Food Sciences, DISAFA, University of Turin, Turin, Italy
[16]Forest Ecology and Forest Management Group, Wageningen University & Research, Wageningen, The Netherlands
[17]Department of Silviculture, Institute of Forest Ecology and Silviculture, University of Agriculture, Krakow, Poland
[18]Centro de Investigação e de Tecnologias Agro-Ambientais e Biológicas, CITAB, Universidade de Trás-os-Montes e Alto Douro, UTAD, Quinta de Prados, 5000-801 Vila Real, Portugal
[19]Universite catholique de Louvain, Faculty of Bioscience Engineering & Earth and Life Institute, Louvain-la-Neuve, Belgium
[20]Faculty of Forestry and Wood Sciences, Czech University of Life Sciences, Prague, Czech Republic
[21]currently at: European Commission, Joint Research Centre, Directorate D – Sustainable Resources - Bio-Economy Unit, via E. Fermi 2749 - TP261, I-21027 Ispra (VA)/Italy
[22]Forest & Nature Lab, Ghent University, Melle-Gontrode, Belgium
[23]Department of Silviculture, Forest Research Institute, Sofia, Bulgaria

*Corresponding author: Swiss Federal Institute of Forest, Snow and Landscape Research WSL, Zürcherstrasse 111, 8903 Birmensdorf, Switzerland, Email: david.forrester@wsl.ch, Phone: +41 (0) 44 739 2869

Keywords; biodiversity; climate; competition; complementarity; forest growth model; mixed-species; silviculture

Summary

The productivity and functioning of mixed-species forests often differs from that of monocultures. However, the magnitude and direction of these differences are difficult to predict because species interactions can be modified by many potentially interacting climatic and edaphic conditions, stand structure and previous management. Process-based forest growth models could potentially be used to disentangle the effects of these factors and thereby improve our understanding of mixed forest functioning while facilitating their design and silvicultural management. However, to date, the predicted mixing effects of forest growth models have not been compared with measured mixing effects. In this study, 26 sites across Europe, each containing a mixture and monocultures of *Fagus sylvatica* and *Pinus sylvestris*, were used to calculate mixing effects on growth and yield and compare them with the mixing effects predicted by the forest growth model 3-PG$_{mix}$. The climate and edaphic conditions, stand structures and ages varied greatly between sites. The model performed well when predicting the stem mass and total mass (and mixing effects on these components), with model efficiency that was usually > 0.7. The model efficiency was lower for growth or smaller components such as foliage mass and root mass. The model was also used to predict how mixing effects would change along gradients in precipitation, temperature, potential available soil water, age, thinning intensity and soil fertility. The predicted patterns were consistent with measurements of mixing effects from published studies. The 3-PG model is a widely used management tool for monospecific stands and this study shows that 3-PG$_{mix}$ can be used to examine the dynamics of mixed-species stands and determine how they may need to be managed.

Introduction

Forest productivity, functioning and stability can differ greatly between mixed-species forests and monocultures. The magnitude and direction of these differences are often uncertain because they are influenced by many potentially interacting factors, including species traits, climatic and edaphic conditions, stand structure and previous management (Forrester, 2014; Bauhus *et al.*, 2017a). Forest growth models are frequently used to predict and disentangle the effects of these factors, which are often occurring and changing simultaneously. When empirical datasets cover an appropriate range in these factors empirical analyses or models can be developed to predict the growth and yield (Mette *et al.*, 2009; Huber *et al.*, 2014; Pretzsch *et al.*, 2015a). However, usually these data do not exist, or the questions being asked are relating to causality, such as *why* a response occurred and not only *how* the forest responded. In this case, process-based models are useful.

Despite the potential of process-based models to predict mixing effects in forests, a recent review found no models that have been tested by comparing the predicted mixing effects with measured mixing effects (Pretzsch *et al.*, 2015b). Therefore, there is an urgent need to test the ability of forest growth models to predict mixing effects. In this study, mixing effects are quantified using the relative productivity (RP); in the form of Equation 1 for the whole mixed stand or Equation 2 for each individual species (Forrester and Pretzsch, 2015).

$$\mathrm{RP}_{total\ stand} = \frac{p_{1,2}}{m_1 p_1 + m_2 p_2} \quad (1)$$

$$\mathrm{RP}_{species\ 1} = \frac{p_{1,(2)}}{m_1 p_1} \quad (2)$$

105

106 The $p_{1,2}$ is the growth or yield of the whole mixture and $p_{1,(2)}$ is the growth or yield of species
107 1 in a mixture with species 2. p_1 and p_2 are the growth or yield of species 1 and species 2 in
108 their respective monocultures. The m_1 and m_2 are the mixing proportions calculated from the
109 basal area of each species. When RP = 1 the growth or yield of the mixtures is exactly as
110 expected based on the monocultures (i.e. an additive effect), indicating no complementarity
111 effect. RP > 1 or RP < 1 indicate overyielding and underyielding effects, respectively, where
112 overyielding occurs when mixtures produce more than the weighted mean of monocultures,
113 and underyielding occurs when mixtures produce less than the weighted mean of
114 monocultures.
115
116 Confidence in the predictions of mixing effects cannot be expected until a given model has
117 been carefully validated. This is more important when modelling mixed-species forests than it
118 is when modelling monocultures because in a mixture, if one species is modelled incorrectly,
119 the predicted competition that species has on all the other species will be incorrectly modelled
120 and any associated bias will build up as the simulation progresses, leading to unrealistic stand
121 dynamics.
122
123 There are at least three criteria that should be used when selecting a model to simulate the
124 dynamics of mixed-species forests. Firstly, the model should simulate the processes and
125 interactions that are likely to be important in the target mixed forest. Some of these are listed
126 in Table 1. While many tree level models can simulate most of these processes (e.g., Maestra;
127 Medlyn, 2004), they often require extensive data for parameterization and operate at high
128 temporal and spatial resolutions, which results in high computational demands. Calculations
129 at high resolutions (e.g. leaves and hours) can also result in errors that are propagated when
130 upscaling, and high resolutions are not necessary when the desired outputs are at lower

131 temporal (months or years) or spatial (stands) resolutions, such as those often required by
132 forest managers. Furthermore, many important processes and interactions shown in Table 1
133 can be calculated at the cohort and stand levels (not only at the tree or leaf levels) (Pretzsch *et*
134 *al.*, 2015b). Therefore, stand level models have been used to reduce computation demands and
135 to avoid the propagation of bias associated with upscaling (e.g., Härkönen *et al.*, 2010;
136 Forrester and Tang, 2016).
137
138 The second criterion is that all processes (e.g., equations or submodels) that the model
139 includes should have been evaluated by comparing predictions against empirical data
140 (Grimm, 1999; Weiskittel *et al.*, 2010), preferably for many different forest types and species.
141 That is, it is easy to achieve a very good fit to observed growth and yield data for the wrong
142 physiological reasons (Sands, 2004). Good predictions of growth and yield do not reliably
143 indicate whether the other calculations (light, water balance, carbon partitioning, nutrient
144 cycling) are accurate or therefore whether the model is reliable.
145
146 The third criterion is that species-specific parameters must not change with species
147 interactions. Species interactions can change the resource availability and within-stand
148 climatic conditions and thereby the physiological performance of a given species, but they
149 cannot change the basic physiology of that species; in other words, the species cannot change
150 into a different species. Therefore, it should be possible to use a single parameter set for a
151 given species (or provenance or clone) to simulate its response to competition, climatic and
152 edaphic factors. For example, single parameter sets for *Acacia* hybrids, *Eucalyptus* hybrids
153 and *Pinus taeda* have been used by the 3-PG model (Physiological Principles Predicting
154 Growth) to simulate their responses across wide ranges of soils, climates and silvicultural
155 treatments (Almeida *et al.*, 2010; Gonzalez-Benecke *et al.*, 2016; Hung *et al.*, 2016). This also

156 enables the use of data from monocultures to parameterize and calibrate models to be used for
157 mixtures when there is no empirical data available for the given mixture.
158
159 The 3-PG model (Landsberg and Waring, 1997) fits these three criteria. However, it has rarely
160 been used for mixed-species forests (Forrester and Tang, 2016). Therefore, the first objective
161 of this study was to (1) examine whether the recently developed mixed species version, 3-
162 PG_{mix}, could predict the growth and yield of *Pinus sylvestris* and *Fagus sylvatica* forests
163 distributed across 26 sites in Europe (Fig. 1), while using single parameter sets for each
164 species. The second objective was to (2) test whether 3-PG_{mix} could predict the mixing effects
165 on the growth and yield of these *Pinus sylvestris* and *Fagus sylvatica* mixtures. Previous
166 studies that used the same plots found large variability in mixing effects, which were weakly
167 correlated with site or climatic variables (Pretzsch *et al.*, 2015a; del Río *et al.*, 2017), although
168 mixing effects for *P. sylvestris* were caused, at least partly, by light-related interactions
169 (Forrester *et al.*, in press). The unclear causality possibly resulted because multiple factors can
170 cause the mixing effects and these cannot be teased apart using empirical data without a
171 higher number of plots or detailed physiological measurements. Therefore, the third objective
172 was (3) to use 3-PG_{mix} to investigate which processes might be causing the mixing effects at
173 the different sites and to examine whether 3-PG_{mix} predicts how mixing effects change along
174 gradients in climate, soil fertility, age and thinning intensity that are consistent with empirical
175 studies about these species. Thinning intensity was considered because this is a main
176 silvicultural treatment that could be used to modulate mixing effects (Bauhus *et al.*, 2017b),
177 and many studies have found that mixing effects can change with stand density (Garber and
178 Maguire, 2004; del Río and Sterba, 2009; Condés *et al.*, 2013; Forrester *et al.*, 2013).
179
180 **Methods**
181

182 *Site description*

183

184 Model predictions were compared with data collected from 26 sites. At each site, there were
185 three plots, including a mixture and monocultures of *P. sylvestris* and *F. sylvatica*. The sites
186 were distributed along a productivity and rainfall gradient through Europe, through much of
187 the overlapping area of the distributions of *P. sylvestris* and *F. sylvatica*. The southernmost
188 sites are located in Spain and Bulgaria and the northernmost sites are in Sweden (Fig. 1). The
189 plots were generally rectangular and ranged in size from 0.037 to 0.462 ha. Plot selection
190 criteria were that they were as close as possible to even-aged, that they had not been thinned
191 for at least ten years and that the trees were mostly mixed on a tree-by-tree basis. The stands
192 were all semi-natural forests as opposed to plantations. In addition, for a given site, all three
193 plots had to be on a similar soil substrate, aspect and slope. The data and a more detailed
194 description of the data are provided in Heym *et al.* (2017) and Heym *et al.* (in press).

195

196 At these locations the mean annual precipitation ranges from 520 to 1,175 mm, the mean
197 temperature from 6.0 to 10.5 °C and the elevation from 20 to 1,339 m a.s.l. A site productivity
198 index (*SI*) was calculated for each species as the height of the 100 largest-diameter trees of
199 that species per hectare in monospecific stands at age 50 years (Pretzsch *et al.*, 2015a). The *SI*
200 ranged from 11.7 to 27.6 m for *F. sylvatica* and from 9.5 to 26.9 m for *P. sylvestris*. More
201 detail about the climatic and edaphic conditions of each site is provided in Table A2 of
202 Appendix A.

203

204 A wide range of stand structures was covered by the 78 plots at the 26 sites. In the mixtures,
205 the percent of basal area that was *P. sylvestris* ranged from 28% to 73%. The basal area
206 ranged from 13.3 to 78.0 m^2 ha^{-1}, the number of trees per hectare from 82 to 2,649 and the
207 stand age from 40 to 150 years.

208

209 *Data collection*

210

211 The diameters at 1.3 m of all trees were measured in each plot. The heights, height to the
212 crown base and crown diameters were also measured for all trees or for a sample of trees (at
213 least 10 randomly selected trees per species per plot). These measurements were conducted
214 between autumn 2013 and spring 2014. Tree dimensions and annual growth for each year
215 from 2002 to 2014 were calculated using increment cores that were collected from at least 20
216 trees per species per plot covering the diameter range for the given species and plot. The
217 diameter increments of all non-cored trees were calculated by fitting diameter increment
218 functions for each plot and species, where diameter increment was a function of diameter at
219 1.3 m and both were log-transformed. More detail is provided in Pretzsch *et al.* (2015a). The
220 crown diameters, heights and live-crown lengths of the trees that were not measured, or for
221 years prior to 2014, were predicted using site- and species-specific allometric equations that
222 were developed in another study using the same plots (Forrester *et al.*, in press). Plot biomass
223 (stems, foliage and roots) was estimated using generalized biomass relationships for *F.*
224 *sylvatica* and *P. sylvestris* that incorporate the effects of stand basal area, trees per ha and age
225 (Forrester *et al.*, 2017b).

226

227 *Description of 3-PG$_{mix}$*

228

229 The 3-PG model was developed by Landsberg and Waring (1997) and since then it has been
230 validated for many species and regions around the world (Landsberg and Sands, 2010). The
231 original version of 3-PG was developed for monocultures but recent modifications have
232 extended its use to mixed-species forests (3-PG$_{mix}$; Forrester and Tang, 2016). The input
233 parameters and their units are listed in Table A1 of Appendix 1 and the types of species

234 interactions that can be simulated are listed in Table 1. The 3-PG$_{mix}$ model has a monthly time
235 step and consists of five sub-models in a causal chain starting with light absorption and
236 assimilation and culminating with the conversion of biomass into output variables commonly
237 used by foresters (Landsberg and Waring, 1997; Sands and Landsberg, 2002). The first sub-
238 model predicts light absorption using the model described in Forrester *et al.* (2014) and then
239 predicts gross primary production (*GPP*) using the maximum potential light-use efficiency
240 (α_{Cx}). The α_{Cx} is reduced in response to limitations imposed by temperature, frost, vapour
241 pressure deficit (*VPD*), soil moisture, soil fertility, atmospheric CO_2 and stand age (Landsberg
242 and Waring, 1997; Sands and Landsberg, 2002; Almeida *et al.*, 2004). Net primary production
243 (*NPP*) is calculated assuming *NPP*/*GPP* = 0.47 (Waring *et al.*, 1998).
244
245 The *NPP* is distributed to foliage, stems and roots by the second sub-model. Soil fertility,
246 *VPD* and soil moisture influence partitioning to roots while partitioning between stems and
247 foliage is influenced by tree size, with larger trees partitioning a lower proportion of *NPP* to
248 foliage (Landsberg and Waring, 1997; Sands and Landsberg, 2002). The third sub-model
249 calculates density-dependent mortality using the -3/2 self-thinning law (Yoda *et al.*, 1963) to
250 adjust the number of trees per ha (Landsberg and Waring, 1997; Sands and Landsberg, 2002).
251 Density-independent mortality can also be predicted (Sands, 2004; Gonzalez-Benecke *et al.*,
252 2014). The water balance is predicted by the fourth sub-model. Canopy conductance g_c is
253 calculated using a species-specific maximum g_c, leaf area index (*LAI*) and any limitations
254 caused by *VPD*, soil moisture, atmospheric CO_2 and stand age. The former two can vary
255 along vertical gradients within the canopy depending on the vertical distribution of foliage.
256 Transpiration and soil evaporation are calculated using the Penman–Monteith equation and
257 these are added to canopy interception to predict evapotranspiration. Soil water is calculated
258 as the difference between evapotranspiration and rainfall, with any water in excess of the
259 maximum soil water holding capacity being drained off (Sands and Landsberg, 2002). If

evapotranspiration is greater than the available soil water, the *NPP* is reduced. The fifth sub-model converts biomass into output variables such as mean tree diameter, height, basal area, wood volume, etc.

The calculation of species mixing proportions is required for several relationships in 3-PG$_{mix}$ and these proportions must be calculated using appropriate variables (Forrester and Tang, 2016). For example, the total stand *LAI* used to calculate canopy interception and canopy conductance is adjusted using mixing proportions based on species contributions to stand *LAI*. Whereas the number of trees per ha (*N*) used for self-thinning calculations is adjusted based on the mixing proportions in terms of stem mass because the equation describing the self-thinning law is based on stem mass.

To simulate the dynamics of deciduous species, two parameters are required that define the month when leaves are produced ($leaf_P$) and the month when they are lost ($leaf_L$) (Forrester and Tang, 2016). Leaves are lost at the beginning of month $leaf_L$ and the foliage biomass (*WF,* Mg ha^{-1}) that was lost at the start of $leaf_L$ will be produced again at the end of month $leaf_P$. At the start of the growing season, all *NPP* is partitioned to *WF* (none to stems *WS* or roots *WR;* both Mg ha^{-1}) until an NPP equal to the *WF* has been produced, and after that, NPP will be partitioned to *WS, WF* and *WR*. For a full description of 3-PG$_{mix}$ please see Forrester and Tang (2016).

Parameterisation

Most parameters were estimated using data collected in the plots and from published studies, as indicated in Table A1 and described below. A small number of parameters were fitted, including those that define biomass partitioning between foliage and stems (p_2, p_{20}), the

minimum and maximum partitioning to roots (η_{Rx} and η_{Rn}) and the litterfall rates (γ_{Fx} and γ_{R}). This model calibration was firstly done using monospecific plots, with 3-PG$_{mix}$ initialised with the stand structure that existed in each plot in 2002 in terms of species-specific age, foliage mass, stem mass, root mass and trees per ha. The 3-PG$_{mix}$ model was then run for 11 years and the predictions for 2013 were compared with the measured values. One parameter was changed at a time until predicted diameter, height, basal area and biomass variables from monocultures were as close as possible to those estimated in the plots.

Meteorological data

The 3-PG$_{mix}$ model requires monthly weather data. This was obtained from the ERA-Interim reanalysis daily data, which was used to provide monthly weather data (from 2002 to 2014) with a spatial resolution of 0.125 ° latitude × 0.125 ° longitude, ≈10 km × 10 km, depending on the latitude (Dee *et al.*, 2011). This is the latest global atmospheric reanalysis dataset produced by the European Centre for Medium-Range Weather Forecasts. The climatic variables included monthly mean daily minimum, maximum and mean temperature, precipitation and solar radiation. The use of ERA-Interim data instead of site-specific data could add some error to the 3-PG$_{mix}$ predictions. No weather stations were located at the sites but solar radiation (the most difficult weather variable to obtain) from weather stations that were close to three of the sites, was highly correlated ($R^2 > 0.7$) with the ERA-Interim data.

Allometric relationships

In contrast to the individual tree allometric relationships described in "*Data collection*", 3-PG$_{mix}$ predicts mean height ($\bar{h}$, m), mean live-crown length ($\bar{h}_L$, m) and mean maximum crown diameter ($\bar{K}$, m) to quantify the canopy structure in order to predict light absorption

and the vertical gradients in climatic conditions within the canopy (Forrester and Tang, 2016). These are predicted in 3-PG$_{mix}$ as functions of mean stem diameter at 1.3 m ($\bar{B}$, cm), relative height (*rh*, height of the target species divided by the mean height of all species in the plot), age (*A*, years) and competition (Equations 3 to 5) and data from the mixed and monospecific plots,

$$ln(h) = ln(a_H) + n_{HB} \times \ln(B) + n_{HC} \times \ln(C) \quad (3)$$

$$ln(h_L) = ln(a_{HL}) + n_{HLB} \times ln(B) + n_{HLrh} \times ln(rh) + n_{HLC} \times \ln(C) \quad (4)$$

$$ln(K) = ln(a_K) + n_{KB} \times \ln(B) + n_{Krh} \times \ln(rh) + n_{KC} \times \ln(C) \quad (5)$$

where all a_x or n_x parameters are constants. The competition index (*C*) is calculated as the sum of the species-specific products of basal area and wood density using Equation 6 (Forrester and Tang, 2016), which is assumed to reflect the current competition in relation to leaf area or sapwood area and hence light, transpiration and metabolic activity (Forrester *et al.*, 2017a).

$$C = \sum_{i=1}^{n} BA_i \times \rho_i \quad (6)$$

where *BA* is the basal area (m^2 ha^{-1}) and ρ is the wood density (g cm^{-3}) of species *i*. The *C* is then expressed per ha after dividing by plot area (m^2).

Equations 3 to 5 were fitted for each species as mixed models, with plot nested within site as the random structure, using the *nlme* package for fitting the mixed models (Harrison *et al.*, 2009) with R 3.2.1 (R Core Team, 2016). To correct for the bias when back-transforming the response variables, a correction factor was calculated as the sum of the measured values divided by the sum of the (back-transformed) predicted values (Snowden, 1991). The back-transformed constants (a_H, a_{HL} and a_K) need to be adjusted by multiplying by the correction factors.

The parameters that describe the relationship between individual tree stem mass w_s and diameter (a_S and n_S) were obtained from Forrester *et al.* (2017b), as were the parameters describing the relationship between age and specific leaf area. The mean wood density was estimated from values found in the literature (*P. sylvestris*; Landsberg *et al.*, 2005; Xenakis *et al.*, 2008) (*F. sylvatica*; Barbaroux, 2002; Cienciala *et al.*, 2005; Gryc *et al.*, 2008; Skovsgaard and Nord-Larsen, 2012). There was no relationship between wood density and age and therefore the wood density was assumed to be constant for each given species, as also assumed in studies where 3-PG was applied to *P. sylvestris* in northern Europe (Landsberg *et al.*, 2005; Xenakis *et al.*, 2008). In this study, the wood density is only used by 3-PG$_{mix}$ to calculate the competition index (Equation 6).

Quantum yield and biomass partitioning

The efficiency with which photosynthetically active radiation (*PAR*) is used to produce biomass (canopy quantum efficiency, α_{Cx}) was estimated by determining the maximum volume growth rates of these species, converting this to *NPP* using wood density and biomass expansion factors (Lehtonen *et al.*, 2004; Vande Walle *et al.*, 2005), adding litterfall estimates based on Lehtonen *et al.* (2004) (not for the deciduous *F. sylvatica*) and converting this to *GPP* assuming a ratio of *NPP*/*GPP* of 0.47 (Waring *et al.*, 1998). This *GPP* was divided by the absorbed *PAR* (*APAR*) based on estimates in the same plots by Forrester *et al.* (in press), which also provided the light extinction coefficient parameters (k_H). The maximum volume growth rates were the maximum current annual increments in yield tables for southwestern Germany (Bösch, 2003), where these species are considered to grow under optimum conditions.

364 The *leaf*$_P$ and *leaf*$_L$ parameters, which describe when deciduous species (*F. sylvatica*) produce
365 and lose their leaves were obtained from local foresters (Table A2 of Appendix A). The
366 temperature limits on α (T_{min}, T_{opt}, T_{max}) were approximations based on San-Miguel-Ayanz *et*
367 *al.* (2016) and Felbermeier and Mosandl (2014) while the default frost effects were used (k_F =
368 1). Maximum stand age parameters of 350 years (*P. sylvestris*) and 300 years (*F. sylvatica*)
369 were applied (Faliński, 1986; Felbermeier and Mosandl, 2014). The default value for the
370 effects of vapour pressure deficit on g_c (k_D) was used for *P. sylvestris* (Landsberg *et al.*, 2005;
371 Xenakis *et al.*, 2008). The k_D for *F. sylvatica* was the mean of values calculated from Jonard
372 *et al.* (2011) and Köcher *et al.* (2009).
373
374 *Self-thinning and size distributions*
375
376 Negligible self-thinning had occurred during the past decade in the plots used in this study.
377 Therefore, the density-dependent mortality parameter, w_{Sx1000}, was set high (400) for each
378 species to prevent any mortality. If required, these parameters can be calculated from previous
379 studies (Pretzsch, 2005; Condés *et al.*, 2017). There was also no evidence or information
380 about density-independent mortality, so these parameters were set at 0.
381
382 The 3-PG$_{mix}$ model uses diameter B (cm) and stem mass w_S (kg) Weibull distributions to
383 correct the bias due to Jensen's Inequality that results from using allometric equations
384 (Forrester and Tang, 2016); the mean of a function is not the same as the function of the mean
385 (Duursma and Robinson, 2003). The location, scale and shape parameters of the Weibull
386 distributions were predicted as functions of mean diameter, relative height (height of the
387 target species divided by the mean height of all trees in the plot), age and the competition
388 index (Equation 6). In the mixtures, the number of trees in each class was adjusted by
389 dividing by the mixing proportion of the given species, based on its contribution to stand

390 basal area. The variables in these equations were log-transformed, which was not the case for
391 the original 3-PG$_{mix}$ model (Forrester and Tang, 2016). The distributions and the Weibull
392 equations are described in Appendix B.
393
394 *Rainfall interception*
395
396 The maximum proportion of rainfall intercepted by the canopy (I_{Rx}) of a given species
397 monoculture was estimated from the mean of values found in the literature for these species
398 (*F. sylvatica*: Nihlgård, 1970; Augusto *et al.*, 2002; Staelens *et al.*, 2006; Staelens *et al.*, 2008;
399 Barbier *et al.*, 2009; Gerrits *et al.*, 2010) (*P. sylvestris*: Rutter, 1963; Gash and Stewart, 1977;
400 Alcock and Morton, 1981; Cape *et al.*, 1991; Augusto *et al.*, 2002; Barbier *et al.*, 2009; Van
401 Nevel, 2015). An *LAI* of 3 for maximum rainfall interception (L_{Ix}) was used based on the
402 patterns shown in the rainfall interception studies cited above that included values of *LAI*.
403
404 *Estimating soil fertility*
405
406 Soil fertility for 3-PG$_{mix}$ is quantified using a fertility rating (FR). When available, site
407 productivity indices and yield tables can provide a good overall estimate of the growing
408 conditions for monocultures. SI indicate the combined effect of different climatic, edaphic
409 and biotic conditions. Therefore, the SI can be described as a function of climate, soil water
410 properties and soil nutrition as shown in Equation 7.
411
412 $$\mathrm{SI} = \beta_0 + \beta_1 \mathrm{ASW} + \beta_2 \mathrm{Martonne} + \varepsilon \quad (7)$$
413
414 where Martonne is the aridity index of each site according to de Martonne (1926), i.e., annual
415 precipitation in mm / (mean annual temperature in °C + 10), which varied from 28 to 61, and

ASW is the potential available soil water (mm). The potential ASW was calculated from the soil depth, the water holding capacity of the given soil`s texture (mm/m) and the proportion of soil volume that is stones. The FR and SI are assumed to represent long-term average conditions and therefore the de Martonne index was calculated from the long-term averages. It was assumed that any variability in SI that was not explained by soil water characteristics (ASW) or climate (de Martonne aridity index) was due to soil fertility and therefore ε provides an index of soil fertility (FR). Therefore, the FR is the observed SI plus the residual, and the residual is the observed SI minus the predicted SI from Equation 7. This was then normalised so that the FR values lie between 0 and 1. Since species interactions can modify soil fertility (Richards *et al.*, 2010), the FR values were only calculated using data from the monocultures, and the resulting FR values were also used in the mixtures. Besides the FR, default parameters for the fertility effects on productivity were used, except for f_{N0}, which describes the lowest relative fertility, namely 0.2 for *P. sylvestris* and 0.5 for *F. sylvatica*.

Evaluation of model performance

To test the light absorption predictions from 3-PG$_{mix}$, its predictions were compared with those from Maestra (Medlyn, 2004), which is a much more detailed tree-level model. Maestra predicts the light absorption of all individual trees within a stand. It uses individual tree positions (x- and y-coordinates), the site slope and individual tree dimensions (crown diameter, length, height and leaf area) to determine the canopy structure and thereby accounts for shading by neighbouring trees. Maestra accounts for intra- or inter-specific differences in crown architecture in terms of crown dimensions, the vertical distribution of leaf-area density, the leaf angle distribution and the optical properties of leaves. The predictions from Maestra were obtained from another study in the same plots that examined how light absorption was influenced by tree allometry, tree size and stand structure (Forrester *et al.*, in press). The

Maestra light absorption predictions compared well with light absorption predicted for the same plots using hemispherical photos, with $R^2 = 0.67$ and a slope (forced through origin) for relationship between observed vs. predicted values of 0.92 (see Fig. S3 in Forrester *et al.*, in press). Maestra light absorption predictions have also been validated in other mixed-species stands (Charbonnier *et al.*, 2013; le Maire *et al.*, 2013). The parameterisation of Maestra for these plots is described in detail in Forrester *et al.* (in press).

The 3-PG_{mix} output variables basal area, stem mass, leaf mass, root mass, diameter, height, APAR and mixing effects (Equations 1 & 2) on these variables were compared with the estimates from the plot measurements (mass variables were calculated using allometric biomass equations, as described above). The model was initialised with the stand structure that existed in each plot in 2002 in terms of species-specific age, foliage mass, stem mass, root mass and trees per ha. It was then run for 11 years and the predictions for 2013 were compared with the measured values. Given that the monospecific plots were used to parameterise and calibrate the model, a validation was performed using the mixed-species plots, before finally combining the data from the mixtures and monocultures to obtain the final parameter set. The criteria used to make comparisons included the relative average error (average bias, *e*%, Equation 8), the relative mean absolute error (MAE%, Equation 9), the mean square error (MSE, Equation 10) (Janssen and Heuberger, 1995; Vanclay and Skovsgaard, 1997) and the model efficiency (EF, Equation 11) (Loague and Green, 1991), which can be less than zero (indicating a poorer model prediction than simply using the mean) up to a maximum of 1, where there is a perfect correlation between predictions and observations.

$$e\% = 100\frac{\tilde{P}-\tilde{O}}{\tilde{O}} \quad (8)$$

$$MAE\% = 100\frac{((\sum_{i=1}^{n}|P_i - O_i|)/n)}{\tilde{O}} \quad (9$$

$$MSE = \frac{\sum_{i=1}^{n}(P_i - O_i)^2}{n} \quad (10)$$

$$EF = \frac{\sum_{i=1}^{n}(O_i - \tilde{O})^2 - \sum_{i=1}^{n}(P_i - O_i)^2}{\sum_{i=1}^{n}(O_i - \tilde{O})^2} \quad (11)$$

where O_i are the observed values, P_i are the predicted values from 3-PG$_{mix}$, and $\tilde{O}$ and $\tilde{P}$ are the means. All statistical analyses were performed using R 3.2.1 (R Core Team, 2016).

Simulation of the spatial and temporal dynamics of species interactions

3-PG$_{mix}$ was then used to simulate the effects of climate, soil fertility, soil water holding capacity, stand age and thinning intensity on mixing effects. To initialise the stands, we used the mean ages, mean species-specific stem mass, root mass, foliage mass and trees per ha in 2002. That is, we used a single "mean" stand structure to initialise all simulations. The final year of the simulations was 2013. A factorial design was used, including 3 species compositions (2 monocultures + 1 mixture) × 6 climates (3 levels of temperature and 3 levels of precipitation) × 6 fertility levels × 6 levels of soil water holding capacity × 4 levels of thinning intensity = 2592 simulations that each went for a duration of 13 years, from age 61 to 73 years (2002 to 2013).

The climates for the temperature gradient were obtained by selecting the climate data from two or three sites with the lowest, medium and highest mean monthly maximum temperatures.

491 Then the mean monthly climate values (from 2002 to 2014) for each given category (low,
492 medium or high) were used to obtain three climatic scenarios with low, medium and high
493 temperatures. A similar procedure was used to obtain three climatic scenarios with low,
494 medium and high annual precipitation. This precipitation gradient also represented a gradient
495 in the terms of the de Martonne (1926) aridity index. Six levels of species-specific soil
496 fertility were used, ranging from the lowest to the highest values calculated for all sites. The
497 fertility was increased for both species simultaneously, because there was a positive
498 correlation between the site productivity indices of each species ($P = 0.017$, $R^2 = 0.25$)
499 (Forrester *et al.*, in press). The 6 levels of maximum available soil water (mm) ranged from 28
500 to 715 mm, which was the range found across the sites in this study. Four thinning intensities
501 were applied at the start of the simulations in 2002 such that 0%, 15%, 30% and 45% of the
502 biomass (of both species) was removed.
503
504 **Results**
505
506 *Validation*
507
508 The *APAR* values predicted by 3-PG$_{mix}$ were well correlated ($R^2 = 0.96$) with predictions from
509 the detailed tree-level model Maestra (Fig. 2). The slope of the regression line fitted to these
510 data and forced through the origin (dashed line in Fig. 2) was 0.978, indicating an average
511 overestimate by 3-PG$_{mix}$ of <3% compared with Maestra. This level of accuracy is relatively
512 high given that the plots covered a wide range of stand structures and leaf area index, and also
513 given that 3-PG$_{mix}$ only uses species-specific means as inputs rather than spatially explicit
514 individual tree information.

515 The 3-PG$_{mix}$ model produced accurate predictions of total biomass, stem mass and anything
516 derived from them such as mean diameter and basal area, which were all highly correlated
517 with the observed values ($R^2 > 0.95$, Fig. 3). For these variables, the predictions for both
518 species were marginally more precise and less biased in the monocultures, which were used
519 for model calibration, than in the mixtures. This was indicated by the mean e% (mono=2.6,
520 mix=3.7), MAE% (mono=15.4, mix=16.4), MSE (mono=789, mix=1 408) and EF
521 (mono=0.72, mix=0.62) (Table 2). The predictions of NPP and stem mass growth were more
522 variable, for example e% was -42.6 to 49.7 in monocultures but -18.5 to -35.8 in mixtures and
523 mean of MAE% was 79 in monocultures and 56 in mixtures. The predictions for growth rates
524 or for variables that had much smaller magnitudes (i.e. foliage and roots), were much less
525 precise (Figs 3 and B3).
526
527 The predicted mixing effects (RP) on growth and yield followed similar patterns for all
528 variables (Table 2). The mixing effects for total biomass, stem mass, basal area and diameter
529 were generally precise (mean MAE% = 13.6) and with a low bias (mean e% = 5.2). In
530 contrast, the predictions of mixing effects for foliage and root mass were not accurate (Fig.
531 B3).
532
533 *Simulations*
534
535 Thinning increased the mixing effects for *P. sylvestris* and the total mixture stem mass (Fig.
536 5f) but reduced mixing effects on *F. sylvatica NPP* (Fig. 6f). Thinning also modified the
537 effect of climate on mixing effects by reducing the differences between species as the
538 thinning intensity increased (Figs 5a,b & 6a,b). For stem mass, this response was more
539 pronounced for *P. sylvestris* than *F. sylvatica*. Increasing soil fertility resulted in higher
540 mixing effects on stem mass for *P. sylvestris* and the total mixture (Fig. 5d) but reduced the

mixing effect on *NPP* for *F. sylvatica* (Fig. 6d). As the stands aged, the mixing effects were predicted to increase for *F. sylvatica* and decline for *P. sylvestris*, with the total mixture showing negligible changes (Fig. 5e & 6e). Drier or hotter climates reduced the mixing effect for *F. sylvatica* but increased the mixing effects for *P. sylvestris* (Figs 5a,b & 6a,b).

Discussion

The 3-PG$_{mix}$ model was able to predict the growth and yield of mixed-species plots after being calibrated using monocultures. It was also able to predict the mixing effects that were consistent with other studies about the same species.

Validation and applicability to the F. sylvatica *and* P. sylvestris *forests of Europe*

The plot network used in this study included a wide range of stand structures and tree allometry, resulting in a correspondingly large range of light regimes (Forrester *et al.*, in press). Even with this complexity, the simple light sub-model of 3-PG$_{mix}$ provided adequate predictions of light absorption. This level of accuracy is acceptable given (i) the variability in stand structures and allometry, (ii) that the comparisons were made against predictions from another model (Maestra) instead of direct measurements of light absorption and (iii) that 3-PG$_{mix}$ at its light sub-model is a stand-level model that simplifies the canopy into cohorts and ignores any spatial clumping of species or trees. Adequate validation of light calculations are critical for the many forest growth models, including 3-PG$_{mix}$, that base their *NPP* calculations on light-use efficiency (McMurtrie *et al.*, 1994; Landsberg and Waring, 1997; Mäkelä *et al.*, 2008), and therefore depend on reliable predictions of light absorption for their growth and yield predictions.

567 3-PG$_{mix}$ accurately predicted biomass yield, basal area and mean tree dimensions at the end of
568 the 11-year simulation period. This is partly evidence that the model was performing well, but
569 also resulted because actual stand structures (as of 2002, stand ages of 30 to 140 years) were
570 used to initialise the simulations, which improves the accuracy of predictions compared to
571 starting with seedlings (Sands and Landsberg, 2002). A much lower precision was obtained
572 for growth or small biomass components, such as roots and foliage, as has also been observed
573 elsewhere (Paul *et al.*, 2007) and is expected due to the small sizes of these biomass
574 components combined with their much greater relative variability (Forrester *et al.*, 2017b).
575
576 Regardless of the size of the biomass components, there are several additional sources of error
577 that should be considered. Firstly, the "observed" biomass data were predicted using
578 allometric equations. These equations were developed using an independent European-wide
579 data set and accounted for age, tree diameter and several stand structural characteristics that
580 probably account for much of the mixing effects on allometry (Forrester *et al.*, 2017a;
581 Forrester *et al.*, 2017b). Nevertheless, they are unlikely to be as accurate as site-specific
582 destructively sampled biomass measurements. For example, in even-aged stands, such as
583 those in this study, growth and foliage mass tend to decline after peaking when the stands are
584 young (Ryan *et al.*, 1997). *F. sylvatica* leaf area index was declining along an age series from
585 80 to 160 years in Germany (Leuschner *et al.*, 2006) and yield tables of southwestern
586 Germany indicate that volume increments decline after peaking at ages 35-45 years for *P.*
587 *sylvestris* and 65-85 years for *F. sylvatica*, with peaks occurring earlier on more productive
588 sites (Bösch, 2003). Given the current ages of these stands (40 to 150 years) the growth rates
589 and foliage mass at many of the sites are likely to be showing long-term trends of decline.
590 Even with age as an independent variable, these tree-level allometric equations may not be
591 precise enough to capture this stand-level variability. 3-PG$_{mix}$ is probably more sensitive to

592 differences in site, age and stand structural conditions than the allometric equations and
593 therefore the error and bias of the 3-PG$_{mix}$ biomass predictions was probably overestimated.
594
595 A second source of error is the potential for genetic variability of the 3-PG$_{mix}$ parameters. The
596 physiology, morphology and phenology of *F. sylvatica* and *P. sylvestris* probably changed
597 along the transect in relation to the different climatic and edaphic conditions (Rehfeldt *et al.*,
598 2002; Robson *et al.*, 2012). That is, the *P. sylvestris* trees in Sweden probably differ to the *P.*
599 *sylvestris* in Spain, but when calculating the parameter values, data from a wide range in the
600 distributions were combined into a mean value for each parameter; there were not enough
601 data to develop region-specific parameter sets. Process-based models are rarely applied across
602 such large natural distributions of a single species and therefore an effect of genetic variability
603 cannot be compared with other studies.
604
605 Most forest growth models, regardless of whether they are empirical or process-based, face
606 the problem of systematic genetic variability (in physiology/morphology/phenology) when
607 applied across an area large enough to include multiple provenances of the given species. This
608 genetic effect could be incorporated into models if the genetic influence on parameters varies
609 systematically with climatic or edaphic conditions, otherwise different parameter sets will be
610 required for each provenance. For example, clone-specific parameter sets are used when
611 applying 3-PG to *Eucalyptus* plantations in south America (e.g., Almeida *et al.*, 2004).
612 Models applied to large areas that ignore systematic differences in physiological,
613 morphological and phenological characteristics of a species may not be reliable for predicting
614 many aspects of forest functioning, including species interactions and potential changes in
615 species distributions. Similarly, parameter sets developed for a given species in one part of its
616 natural distribution may not be reliable for the same species in another part of its natural
617 distribution. The general European-wide parameters used in this study should be further

refined when applied to specific regions. This refinement should target the parameters that are most likely to change and that 3-PG$_{mix}$ is most sensitive too, such as p_{20}, k_H, α_{Cx}, σ_1 (Forrester and Tang, 2016).

This does not mean that a single parameter set cannot be applied to large areas with wide ranges in climatic and edaphic conditions. For example, 3-PG is well known to provide very precise and less biased predictions using a single parameter set, when the genetic variability of the simulated species is relatively low, such as in plantations, even when the growing conditions span a wide range of climates, soil types and silvicultural treatments (Almeida *et al.*, 2010; Gonzalez-Benecke *et al.*, 2016; Hung *et al.*, 2016). 3-PG has also already been shown to provide accurate predictions for *P. sylvestris* in northern Europe using parameters similar to those used in this study (Landsberg *et al.*, 2005; Xenakis *et al.*, 2008), and other stand-level forest growth models have also performed well using single parameter sets (Härkönen *et al.*, 2010).

Comparison of simulations with published empirical observations

3-PG$_{mix}$ was designed specifically to include many of the species interactions that can influence the growth and functioning of mixed-species forests (Table 1). Even though it does not include all possible species interactions and all interactions are simulated at the stand level (not at the tree level), the predicted mixing effects compared well with the observed mixing effects at the 26 sites used for this study which covered a wide range in stand structures and climates. This suggests that the most influential processes driving the dynamics of these forests are included in 3-PG$_{mix}$ (Table 1). The predictions also compared well with other studies about these species. For example, as thinning intensity increased, the mixing effects were predicted to decline for *F. sylvatica* but increase for *P. sylvestris*. This pattern was also

found in response to differences in stand density using a large dataset from Spain (Condés *et al.*, 2013).

As soil fertility increased, the mixing effect was predicted to increase for *P. sylvestris*. Increasing mixing effects with increasing soil fertility are likely to result when species interactions improve light absorption or light-use efficiency (Forrester, 2014). Consistent with this prediction, another study that used the same plots found that the mixing effects for *P. sylvestris* growth were correlated with mixing effects on light absorption (Forrester *et al.*, in press).

As the stands aged, the mixing effects were predicted to increase for *F. sylvatica* and decline for *P. sylvestris*. At the start of the simulation, age 62 years, the mean height of *P. sylvestris* was 21.5 m and *F. sylvatica* was 15.6 m, but by the end of the simulation at age 73 years, the height difference was much smaller (22.7 and 20.7 m, respectively). Therefore, the vertical overlap between *F. sylvatica* and *P. sylvestris* crowns increased, which probably reduced the light complementarity effect experienced by *P. sylvestris*. This highlights the potential need for thinning *F. sylvatica* from the larger size classes to maintain the upper canopy position of *P. sylvestris* (Spathelf and Ammer, 2015). It is also important to note that the initial conditions used as inputs for 3-PG$_{mix}$ (e.g. species specific values of trees per hectare, biomass per ha, age) will influence the simulation. The mean conditions of all sites were used in this study in order to examine general patterns. However, if the actual dynamics for specific sites are of interest, then site-specific inputs are required. Similarly, the simulation in this study ran for 11 years, but a more reliable test could include a greater proportion of the rotation.

669 The effects of climate were also consistent with those reported in the literature. 3-PG$_{mix}$
670 predicted that mixing effects for *F. sylvatica* would be lowest at dry or hot sites, while those
671 for *P. sylvestris* would be highest on those sites. This is consistent with a Spanish study on the
672 same species (Condés and Río, 2015).
673
674 *Conclusions*
675
676 To our knowledge, this is the first time a forest growth model has been validated for its ability
677 to predict mixing effects using empirical measurements of the mixing effects. This is despite
678 the fact that most forests are mixed and that forest growth models are often applied to mixed-
679 species forests. 3-PG$_{mix}$ predicted standing biomass well and predicted changes in mixing
680 effects in response to soils, stand density, climate and age that matched measured data and
681 case studies from the literature. Growth predictions were less precise than yield predictions,
682 probably partly because the "observed" data were predicted using biomass equations (as
683 opposed to more direct measurements) and because the parameter set was general for Europe
684 and not site-specific.
685
686 Previous studies using the same plots found few clear spatial changes in mixing along the
687 transect (Pretzsch *et al.*, 2015a; del Río *et al.*, 2017), except that the mixing effect on *P.*
688 *sylvestris* growth was caused by light-related interactions (Forrester *et al.*, in press). The
689 difficulty in identifying significant patterns in previous studies was probably because multiple
690 factors and processes influenced the mixing effects, and even with more than 30 sites (90
691 plots) distributed across Europe, it was not possible to disentangle these factors to show which
692 processes were driving the mixing effects. 3-PG$_{mix}$ was used to tease apart the effect of
693 climates, age and densities or thinning regimes on mixing effects and could therefore be used

694 to identify which processes may have caused the mixing effects and which sites, may be
695 suitable or unsuitable for mixtures (Figs 6 and 7).
696
697 Models such as 3-PG$_{mix}$ can be used to get an impression of the main processes and species
698 interactions that drive mixing effects in forests and can facilitate the development of
699 hypotheses, experimental designs and aid silvicultural decisions. Similarly, 3-PG$_{mix}$ could also
700 be used to determine how experiments might need to be managed in the future, such as
701 whether some species will need to be thinned to prevent them from dominating the other
702 species or to maintain mixing effects at high levels.
703
704 **Acknowledgements**
705
706 This article is based upon work from COST Action EuMIXFOR, supported by COST
707 (European Cooperation in Science and Technology). Funding for the Czech Republic site was
708 provided by the MŠMT projects COST CZ - LD14063 and LD14074. All contributors thank
709 their national funding institutions and the forest owners for agreeing to establish the triplets
710 and to measure and analyse data from the triplets. The first author was funded by a
711 Heisenberg Fellowship (FO 791/4-1) from the German Research Foundation (Deutsche
712 Forschungsgemeinschaft, DFG). Mário Pereira was supported by the project Interact -
713 Integrative Research in Environment, Agro-Chain and Technology, NORTE-01-0145-
714 FEDER-000017, research line BEST, co-financed by FEDER/NORTE 2020.
715
716 **References**
717
718 Alcock, M.R., Morton, A.J., 1981. The sulphur content and pH of rainfall and throughfall
719 under pine and birch. Journal of Applied Ecology 18, 835-839.

720 Almeida, A.C., Siggins, A., Batista, T.R., Beadle, C., Fonseca, S., Loos, R., 2010. Mapping
721 the effect of spatial and temporal variation in climate and soils on *Eucalyptus* plantation
722 production with 3-PG, a process-based growth model. Forest Ecology and Management
723 259, 1730-1740.
724 Almeida, A.C.d., Landsberg, J.J., Sands, P.J., 2004. Parameterisation of 3-PG model for fast-
725 growing *Eucalyptus grandis* plantations. Forest Ecology and Management 193, 179-
726 195.
727 Augusto, L., Ranger, J., Binkley, D., Rothe, A., 2002. Impact of several common tree species
728 of European temperate forests on soil fertility. Annals of Forest Science 59, 233-253.
729 Barbaroux, C., 2002. Analyse et modélisation des flux de carbone de peuplements forestiers
730 pour la compréhension de la croissance de deux espèces feuillues *Quercus petraea* et
731 *Fagus sylvatica*, PhD thesis. University of Paris-Sud, Orsay, France, 178.
732 Barbier, S., Balandier, P., Gosselin, F., 2009. Influence of several tree traits on rainfall
733 partitioning in temperate and boreal forests: a review. Annals of Forest Science 66, 602.
734 Bauhus, J., Forrester, D.I., Gardiner, B., Jactel, H., Vallejo, R., Pretzsch, H., 2017a.
735 Ecological stability of mixed-species forests. In: Pretzsch, H., Forrester, D.I., Bauhus, J.
736 (Eds.), Mixed-Species Forests, Ecology and Management. Springer-Verlag Berlin
737 Heidelberg, pp. 339-384.
738 Bauhus, J., Forrester, D.I., Pretzsch, H., Felton, A., Pyttel, P., Benneter, A., 2017b.
739 Silvicultural options for mixed-species stands. In: Pretzsch, H., Forrester, D.I., Bauhus,
740 J. (Eds.), Mixed-Species Forests, Ecology and Management. Springer-Verlag Berlin
741 Heidelberg, pp. 435-503.
742 Bösch, B., 2003. Neue Schätzhilfen für Wuchsleistungen der Hauptbaumarten (New guide
743 curves for the assessment of the growth potential of the main tree species in Baden-
744 Wuerttemberg). Forstliche Versuchs- und Forschungsanstalt Baden-Württemberg. 12 p.

745 Cape, J.N., Brown, A.H.F., Robertson, S.M.C., Howson, G., Paterson, I.S., 1991. Interspecies
746 comparisons of throughfall and stemflow at three sites in northern Britain Forest
747 Ecology and Management 46, 165-177.
748 Charbonnier, F., Maire, G.l., Dreyer, E., Casanoves, F., Christina, M., Dauzat, J., Eitel,
749 J.U.H., Vaast, P., Vierling, L.A., Roupsard, O., 2013. Competition for light in
750 heterogeneous canopies: Application of MAESTRA to a coffee (*Coffea arabica* L.)
751 agroforestry system. Agricultural and Forest Meteorology 181, 152-169.
752 Cienciala, E., Cerny, M., Alptauer, J., Exnerova, Z., 2005. Biomass functions applicable to
753 European beech. Journal of Forest Science 51, 147-154.
754 Condés, S., Río, M.d., 2015. Climate modifies tree interactions in terms of basal area growth
755 and mortality in monospecific and mixed *Fagus sylvatica* and *Pinus sylvestris* forests.
756 European Journal of Forest Research 134, 1095-1108.
757 Condés, S., Río, M.d., Sterba, H., 2013. Mixing effect on volume growth of *Fagus sylvatica*
758 and *Pinus sylvestris* is modulated by stand density. Forest Ecology and Management
759 292, 86-95.
760 Condés, S., Vallet, P., Bielak, K., Bravo-Oviedo, A., Coll, L., Ducey, M.J., Pach, M.,
761 Pretzsch, H., Sterba, H., Vayreda, J., Río, M.d., 2017. Climate influences on the
762 maximum size-density relationship in Scots pine (*Pinus sylvestris* L.) and European
763 beech (*Fagus sylvatica* L.) stands. Forest Ecology and Management 385, 295-307.
764 Dee, D.P., Uppala, S.M., Simmons, A.J., Berrisford, P., Poli, P., Kobayashi, S., Andrae, U.,
765 Balmaseda, M.A., Balsamo, G., Bauer, P., Bechtold, P., Beljaars, A.C.M., Berg, L.v.d.,
766 Bidlot, J., Bormann, N., Delsol, C., Dragani, R., Fuentes, M., Geer, A.J., Haimberger,
767 L., Healy, S.B., Hersbach, H., Hólm, E.V., Isaksen, L., Kållberg, P., Köhler, M.,
768 Matricardi, M., McNally, A.P., Monge-Sanz, B.M., Morcrette, J.-J., Park, B.-K.,
769 Peubey, C., Rosnay, P.d., Tavolato, C., Thépaut, J.-N., Vitart, F., 2011. The ERA-

770 Interim reanalysis: configuration and performance of the data assimilation system.
771 Quarterly Journal of the Royal Meteorological Society 137, 553-597.
772 del Río, M., Pretzsch, H., Ruíz-Peinado, R., Ampoorter, E., Annighöfer, P., Barbeito, I.,
773 Bielak, K., Brazaitis, G., Coll, L., Drössler, L., Fabrika, M., Forrester, D.I., Heym, M.,
774 Hurt, V., Kurylyak, V., Löf, M., Lombardi, F., Madrickiene, E., Matović, B., Mohren,
775 F., Motta, R., den Ouden, J., Pach, M., Ponette, Q., Schütze, G., Skrzyszewski, J.,
776 Sramek, V., Sterba, H., Stojanović, D., Svoboda, M., Zlatanov, T., Bravo-Oviedo, A.,
777 2017. Species interactions increase the temporal stability of community productivity in
778 *Pinus sylvestris-Fagus sylvatica* mixtures across Europe. Journal of Ecology 105, 1032-
779 1043.
780 del Río, M., Sterba, H., 2009. Comparing volume growth in pure and mixed stands of *Pinus*
781 *sylvestris* and *Quercus pyrenaica*. Annals of Forest Science 66, 502.
782 Duursma, R.A., Robinson, A.P., 2003. Bias in the mean tree model as a consequence of
783 Jensen's inequality. Forest Ecology and Management 186, 373-380.
784 Faliński, J.B., 1986. Vegetation dynamics in temperate lowland Primeval Forests. Ecological
785 Studies in Białowieża Forest. Dr W. Junk Publishers, Dordrecht. 537 p.
786 Felbermeier, B., Mosandl, R., 2014. Fagus sylvatica. In, Enzyclopädie der Holzgewächse.
787 Wiley-VCH Verlag.
788 Forrester, D.I., 2014. The spatial and temporal dynamics of species interactions in mixed-
789 species forests: From pattern to process. Forest Ecology and Management 312, 282-292.
790 Forrester, D.I., Ammer, C., Annighöfer, P.J., Barbeito, I., Bielak, K., Bravo-Oviedo, A., Coll,
791 L., Río, M.d., Drössler, L., Heym, M., Hurt, V., Löf, M., Ouden, J.d., Pach, M., Pereira,
792 M.G., Plaga, B., Ponette, Q., Skrzyszewski, J., Sterba, H., Svoboda, M., Zlatanov, T.,
793 Pretzsch, H., in press. Effects of crown architecture and stand structure on light
794 absorption in mixed and monospecific *Fagus sylvatica* and *Pinus sylvestris* forests
795 along a productivity and climate gradient through Europe. Journal of Ecology.

796 Forrester, D.I., Bauhus, J., 2016. A review of processes behind diversity - productivity
797 relationships in forests. Current Forestry Reports 2, 45-61.
798 Forrester, D.I., Benneter, A., Bouriaud, O., Bauhus, J., 2017a. Diversity and competition
799 influence tree allometry - developing allometric functions for mixed-species forests.
800 Journal of Ecology 105, 761-774.
801 Forrester, D.I., Guisasola, R., Tang, X., Albrecht, A.T., Dong, T.L., le Maire, G., 2014. Using
802 a stand-level model to predict light absorption in stands with vertically and horizontally
803 heterogeneous canopies. Forest Ecosystems 1, 17.
804 Forrester, D.I., Kohnle, U., Albrecht, A.T., Bauhus, J., 2013. Complementarity in mixed-
805 species stands of *Abies alba* and *Picea abies* varies with climate, site quality and stand
806 density. Forest Ecology and Management 304, 233-242.
807 Forrester, D.I., Pretzsch, H., 2015. Tamm Review: On the strength of evidence when
808 comparing ecosystem functions of mixtures with monocultures. Forest Ecology and
809 Management 356, 41-53.
810 Forrester, D.I., Tachauer, I.H.H., Annighoefer, P., Barbeito, I., Pretzsch, H., Ruiz-Peinado, R.,
811 Stark, H., Vacchiano, G., Zlatanov, T., Chakraborty, T., Saha, S., Sileshi, G.W., 2017b.
812 Generalized biomass and leaf area allometric equations for European tree species
813 incorporating stand structure, tree age and climate. Forest Ecology and Management
814 396, 160-175.
815 Forrester, D.I., Tang, X., 2016. Analysing the spatial and temporal dynamics of species
816 interactions in mixed-species forests and the effects of stand density using the 3-PG
817 model. Ecological Modelling 319, 233-254.
818 Garber, S.M., Maguire, D.A., 2004. Stand productivity and development in two mixed-
819 species spacing trials in the Central Oregon Cascades. Forest Science 50, 92-105.
820 Gash, J.H.C., Stewart, J.B., 1977. The evaporation from Thetford Forest during 1975. Journal
821 of Hydrology 35, 385-396.

822 Gerrits, A.M.J., Pfister, L., Savenije, H.H.G., 2010. Spatial and temporal variability of canopy
823 and forest floor interception in a beech forest. Hydrological Processes 24, 3011-3025.
824 Gonzalez-Benecke, C.A., Jokela, E.J., Cropper Jr, W.P., Bracho, R., Leduc, D.J., 2014.
825 Parameterization of the 3-PG model for *Pinus elliottii* stands using alternative methods
826 to estimate fertility rating, biomass partitioning and canopy closure. Forest Ecology and
827 Management 327, 55-75.
828 Gonzalez-Benecke, C.A., Teskey, R.O., Martin, T.A., Jokela, E.J., Fox, T.R., Kane, M.B.,
829 Noormets, A., 2016. Regional validation and improved parameterization of the 3-PG
830 model for *Pinus taeda* stands. Forest Ecology and Management 361, 237-256.
831 Grimm, V., 1999. Ten years of individual-based modelling in ecology: what have we learned
832 and what could we learn in the future? Ecological Modelling 115, 129-148.
833 Gryc, V., Vavrčík, H., Gomola, Š., 2008. Selected properties of European beech (*Fagus*
834 *sylvatica* L.). Journal of Forest Science 54, 418-425.
835 Härkönen, S., Pulkkinen, M., Duursma, R., Mäkelä, A., 2010. Estimating annual GPP, NPP
836 and stem growth in Finland using summary models. Forest Ecology and Management
837 259, 524-533.
838 Harrison, R.B., Terry, T.A., Licata, C.W., Flaming, B.L., Meade, R., Guerrini, I.A., Strahm,
839 B.D., Xue, D., Lolley, M.R., Sidell, A.R., Wagoner, G.L., Briggs, D., Turnblom, E.C.,
840 2009. Biomass and stand characteristics of a highly productive mixed Douglas-fir and
841 western hemlock plantation in coastal Washington. Western Journal of Applied Forestry
842 24, 180-186.
843 Heym, M., Ruíz-Peinado, R., del Río, M., Bielak, K., Forrester, D.I., Dirnberger, G., Barbeito,
844 I., Brazaitis, G., Ruškytė, I., Coll, L., Fabrika, M., Drössler, L., Löf, M., Sterba, H.,
845 Hurt, V., Kurylyak, V., Lombardi, F., Stojanović, D., Ouden, J.d., Motta, R., Pach, M.,
846 Skrzyszewski, J., Ponette, Q., de Streel, G., Sramek, V., Čihák, T., Zlatanov, T.M.,
847 Avdagic, A., Ammer, C., Verheyen, K., Włodzimierz, B., Bravo-Oviedo, A., Pretzsch,

H., 2017. Data from: EuMIXFOR empirical forest mensuration and ring width data from pure and mixed stands of Scots pine (*Pinus sylvestris* L.) and European beech (*Fagus sylvatica* L.) through Europe. Dryad Digital Repository. doi:10.5061/dryad.8v04m.

Heym, M., Ruíz-Peinado, R., del Río, M., Bielak, K., Forrester, D.I., Dirnberger, G., Barbeito, I., Brazaitis, G., Ruškytė, I., Coll, L., Fabrika, M., Drössler, L., Löf, M., Sterba, H., Hurt, V., Kurylyak, V., Lombardi, F., Stojanović, D., Ouden, J.d., Motta, R., Pach, M., Skrzyszewski, J., Ponette, Q., de Streel, G., Sramek, V., Čihák, T., Zlatanov, T.M., Avdagic, A., Ammer, C., Verheyen, K., Włodzimierz, B., Bravo-Oviedo, A., Pretzsch, H., in press. EuMIXFOR empirical forest mensuration and ring width data from pure and mixed stands of Scots pine (*Pinus sylvestris* L.) and European beech (*Fagus sylvatica* L.) through Europe. Annals of Forest Science.

Huber, M.O., Sterba, H., Bernhard, L., 2014. Site conditions and definition of compositional proportion modify mixture effects in *Picea abies - Abies alba* stands. Canadian Journal of Forest Research 44, 1281-1291.

Hung, T.T., Almeida, A.C., Eyles, A., Mohammed, C., 2016. Predicting productivity of *Acacia* hybrid plantations for a range of climates and soils in Vietnam. Forest Ecology and Management 367, 97-111.

Janssen, P.H.M., Heuberger, P.S.C., 1995. Calibration of process-oriented models. Ecological Modelling 83, 55-66.

Jonard, F., André, F., Ponette, Q., Vincke, C., Jonard, M., 2011. Sap flux density and stomatal conductance of European beech and common oak trees in pure and mixed stands during the summer drought of 2003. Journal of Hydrology 409, 371-381.

Köcher, P., Gebauer, T., VivianaHorna, Leuschner, C., 2009. Leaf water status and stem xylem flux in relation to soil drought in five temperate broad-leaved tree species with contrasting water use strategies. Annals of Forest Science 66, 101.

874 Landsberg, J., Mäkelä, A., Sievänen, R., Kukkola, M., 2005. Analysis of biomass
875 accumulation and stem size distributions over long periods in managed stands of *Pinus*
876 *sylvestris* in Finland using the 3-PG model. Tree Physiology 25, 781-792.
877 Landsberg, J., Sands, P., 2010. Physiological ecology of forest production: Principles,
878 processes and models. Elsevier, Amsterdam. 352 p.
879 Landsberg, J.J., Waring, R.H., 1997. A generalised model of forest productivity using
880 simplified concepts of radiation-use efficiency, carbon balance and partitioning. Forest
881 Ecology and Management 95, 209-228.
882 le Maire, G., Nouvellon, Y., Christina, M., Ponzoni, F.J., Gonçalves, J.L.M., Bouillet, J.-P.,
883 Laclau, J.-P., 2013. Tree and stand light use efficiencies over a full rotation of single-
884 and mixed-species *Eucalyptus grandis* and *Acacia mangium* plantations. Forest Ecology
885 and Management 288, 31-42.
886 Lehtonen, A., Mäkipää, R., Heikkinen, J., Sievänen, R., Liski, J., 2004. Biomass expansion
887 factors (BEFs) for Scots pine, Norway spruce and birch according to stand age for
888 boreal forests. Forest Ecology and Management 188, 211-224.
889 Leuschner, C., Voß, S., Foetzki, A., Clases, Y., 2006. Variation in leaf area index and stand
890 leaf mass of European beech across gradients of soil acidity and precipitation. Plant
891 Ecology 186, 247-258.
892 Loague, K., Green, R.E., 1991. Statistical and graphical methods for evaluating transport
893 models: overview and application. Journal of Contaminant Hydrology 7, 51-73.
894 Mäkelä, A., Pulkkinen, M., Kolari, P., Lagergren, F., Berbigier, P., Lindroth, A., Loustau, D.,
895 Nikinmaa, E., Vesala, T., Hari, P., 2008. Developing an empirical model of stand GPP
896 with the LUE approach: analysis of eddy covariance data at five contrasting conifer
897 sites in Europe. Global Change Biology 14, 92-108.
898 Martonne, E., 1926. Une Nouvelle Fonction CIimatologique: L'Indice d'Aridite (A New
899 CIimatological Function: The Aridity Index). La Météorologie 2, 449-458.

McMurtrie, R.E., Gholz, H.L., Linder, S., Gower, S.T., 1994. Climatic factors controlling the productivity of pine stands: a model-based analysis. Ecological Bulletins 43, 173-188.

Medlyn, B.E., 2004. A MAESTRO Retrospective. In: Mencuccini, M., Moncrieff, J., McNaughton, K., Grace, J. (Eds.), Forests at the Land-Atmosphere Interface. CABI Publishing, Wallingford UK, pp. 105-122.

Mette, T., Albrecht, A., Ammer, C., Biber, P., Kohnle, U., Pretzsch, H., 2009. Evaluation of the forest growth simulator SILVA on dominant trees in mature mixed Silver fir-Norway spruce stands in South-West Germany. Ecological Modelling 220, 1670-1680.

Nanang, D.M., 1998. Suitability of the Normal, Log-normal and Weibull distributions for fitting diameter distributions of neem plantations in Northern Ghana. Forest Ecology and Management 103, 1-7.

Nihlgård, B., 1970. Precipitation, its chemical composition and effect on soil water in a Beech and a Spruce forest in south Sweden. Oikos 21, 208-217.

Paul, K.I., Booth, T.H., Jovanovic, T., Sands, P.J., Morris, J.D., 2007. Calibration of the forest growth model 3-PG to eucalypt plantations growing in low rainfall regions of Australia. Forest Ecology and Management 243, 237-247.

Pretzsch, H., 2005. Link between the self-thinning rules for herbaceous and woody plants. Scientia agriculturae Bohemica 36, 98-107.

Pretzsch, H., del Río, M., Ammer, C., Avdagic, A., Barbeito, I., Bielak, K., Brazaitis, G., Coll, L., Dirnberger, G., Drössler, L., Fabrika, M., Forrester, D.I., Godvod, K., Heym, M., Hurt, V., Kurylyak, V., Löf, M., Lombardi, F., Matović, B., Mohren, F., Motta, R., den Ouden, J., Pach, M., Ponette, Q., Schütze, G., Schweig, J., Skrzyszewski, J., Sramek, V., Sterba, H., Stojanović, D., Svoboda, M., Vanhellemont, M., Verheyen, K., Wellhausen, K., Zlatanov, T., Bravo-Oviedo, A., 2015a. Growth and yield of mixed versus pure stands of Scots pine (*Pinus sylvestris* L.) and European beech (*Fagus*

925 *sylvatica* L.) analysed along a productivity gradient through Europe. European Journal
926 of Forest Research 134, 927-947.
927 Pretzsch, H., Forrester, D.I., Rötzer, T., 2015b. Representation of species mixing in forest
928 growth models. A review and perspective. Ecological Modelling 313, 276-292.
929 R Core Team, 2015. R: A language and environment for statistical computing. R Foundation
930 for Statistical Computing, Vienna, Austria. URL http://www.R-project.org/. p.
931 R Core Team, 2016. R: A language and environment for statistical computing. R Foundation
932 for Statistical Computing, Vienna, Austria. URL http://www.R-project.org/. p.
933 Rehfeldt, G.E., Tchebakova, N.M., Parfenova, Y.I., Wykoff, W.R., Kuzmina, N.A., Milyutin,
934 L.I., 2002. Intraspecific responses to climate in *Pinus sylvestris*. Global Change Biology
935 8, 912-929.
936 Richards, A.E., Forrester, D.I., Bauhus, J., Scherer-Lorenzen, M., 2010. The influence of
937 mixed tree plantations on the nutrition of individual species: a review. Tree Physiology
938 30, 1192-1208.
939 Robson, T.M., Sánchez-Gómez, D., Cano, F.J., Aranda, I., 2012. Variation in functional leaf
940 traits among beech provenances during a Spanish summer reflects the differences in
941 their origin. Tree Genetics & Genomes 8, 1111-1121.
942 Rutter, A.J., 1963. Studies in the water relations of *Pinus sylvestris* in plantation conditions. I.
943 Measurements of rainfall and interception. Journal of Ecology 51, 165-184.
944 Ryan, M.G., Binkley, D., Fownes, J.H., 1997. Age-Related Decline in Forest Productivity:
945 Pattern and Process. Advances in Ecological Research 27, 213-262.
946 San-Miguel-Ayanz, J., de Rigo, D., Caudullo, G., Houston Durrant, T., Mauri, A., 2016.
947 European Atlas of Forest Tree Species. Publication Office of the European Union,
948 Luxembourg p.

949 Sands, P., 2004. Adaptation of 3-PG to novel species: guidelines for data collection and
950 parameter assignment. Technical Report No.141. CRC for Sustainable Production
951 Forestry, 35 p. p.
952 Sands, P.J., Landsberg, J.J., 2002. Parameterisation of 3-PG for plantation grown *Eucalyptus*
953 *globulus*. Forest Ecology and Management 163, 273-292.
954 Skovsgaard, J.P., Nord-Larsen, T., 2012. Biomass, basic density and biomass expansion
955 factor functions for European beech (*Fagus sylvatica* L.) in Denmark. European Journal
956 of Forest Research 131, 1035-1053.
957 Snowden, P., 1991. A ratio estimator for bias correction in logarithmic regressions. Canadian
958 Journal of Forest Research 21, 720-724.
959 Spathelf, P., Ammer, C., 2015. Forest management of Scots pine (*Pinus sylvestris* L.) in
960 northern Germany - A brief review of the history and current trends. Forstarchiv 86, 59-
961 66.
962 Staelens, J., Schrijver, A.D., Verheyen, K., Verhoest, N.E.C., 2006. Spatial variability and
963 temporal stability of throughfall water under a dominant beech (*Fagus sylvatica* L.) tree
964 in relationship to canopy cover. Journal of Hydrology 330, 651-662.
965 Staelens, J., Schrijver, A.D., Verheyen, K., Verhoest, N.E.C., 2008. Rainfall partitioning into
966 throughfall, stemflow, and interception within a single beech (*Fagus sylvatica* L.)
967 canopy: influence of foliation, rain event characteristics, and meteorology. Hydrological
968 Processes 22, 33-45.
969 Van Nevel, L., 2015. Tree species effects on Cd and Zn mobility after afforestation of
970 contaminated soils in the Campine region (northern Belgium).
971 Vanclay, J.K., Skovsgaard, J.P., 1997. Evaluating forest growth models. Ecological
972 Modelling 98, 1-12.

973 Vande Walle, I., van Camp, N., Perrin, D., Lemeur, R., Verheyen, K., van Wesemael, B.,
974 Laitat, E., 2005. Growing stock-based assessment of the carbon stock in Belgian forest
975 biomass. Annals of Forest Science 62, 853-864.
976 Waring, R.H., Landsberg, J.J., Williams, M., 1998. Net primary production of forests: a
977 constant fraction of gross primary production. Tree Physiology 18, 129-134.
978 Weiskittel, A.R., Maguire, D.A., Monserud, R.A., Johnson, G.P., 2010. A hybrid model for
979 intensively managed Douglas-fir plantations in the Pacific Northwest, USA. European
980 Journal of Forest Research 129, 325-338.
981 Xenakis, G., Ray, D., Mencuccini, M., 2008. Sensitivity and uncertainty analysis from a
982 coupled 3-PG and soil organic matter decomposition model. Ecological Modelling 219,
983 1-16.
984 Yoda, K., Kira, T., Ogawa, H., Hozami, K., 1963. Self thinning in overcrowded pure stands
985 under cultivated and natural conditions. Journal of Biology Osaka City University 14,
986 107-129.

987

Table 1. Major processes or species interactions that can influence the growth of mixtures compared with monocultures, modified from Forrester and Bauhus (2016), and whether they can be simulated using the 3-PG$_{mix}$ model. The "Manual" label in the middle column indicates that the process can be simulated by inputting a time series of values for the relevant parameter to reflect its temporal change, based on the user's knowledge of that process, e.g., if rates of nitrogen fixation change, then the fertility parameters may need to change through time.

Name of process or pattern	Presence in 3-PG$_{mix}$	Notes
Nutrient-related		
Symbiotic nitrogen fixation	Manual	Can be simulated manually by changing the fertility rating when the timing and magnitude of the change is known. Or by linking 3-PG$_{mix}$ with a nutrient model (e.g, Xenakis *et al.*, 2008).
Nutrient cycling	Manual	
Chemical, spatial or temporal stratification	Manual	
Nutrient mineralization	Manual	
Canopy nitrogen retention	Manual	
Light-related		
Space occupation – canopy stratification	Yes	
Space occupation – complementary crown shapes and architectures	Yes	Shapes are limited to cones, ellipsoids, half-ellipsoids and boxes.
Space occupation – intra-specific variability in crown architecture and size, or influence of inter-specific competition on intra-specific variability	Yes	Variability in crown architecture via parameters for height, live-crown length and crown diameter equations.
Physiological differences	Yes	e.g. light-use efficiency can be reduced relative to the species potential (α_{Cx}) in response to mixing effects on within canopy vapour pressure deficit, soil moisture and soil fertility.
Phenology and inter-specific effects on these	Manual	Simulated by changing the parameters determining leaf fall and bud break
Water-related		
Hydraulic redistribution	Manual	By using the irrigation silvicultural treatment or changing the available soil water during the simulation
Shared mycorrhizal networks	No	
Canopy interception	Yes	
Transpiration and water-use efficiency	Yes	
Litter layer as a sponge or barrier	Manual	By using the irrigation silvicultural treatment or changing the available soil water during the simulation
Isohydric vs. Anisohydric	Yes	e.g. via the parameter defining stomatal responses to vapour pressure deficit (k_D)
Inter-and intra-specific differences in phenology	Manual	Simulated by changing the parameters determining leaf fall and bud break
Modified within-stand environmental conditions	Yes	
Biotic		
Insect herbivory and leaf pathogens	Manual	e.g. by using the pruning silvicultural treatment or changing the foliage biomass
Other		
Carbon partitioning	Yes	Mixing effects on partitioning to roots relative to aboveground growth occur via changes in soil fertility, vapour pressure

	deficit within the canopy and soil moisture, while partitioning between stems and foliage is related to mixing effects on tree size (larger trees partition a lower proportion of NPP to foliage).

Table 2. Statistical information that describes the relationships between the predicted and observed variables for mixtures (plain font) or monocultures (bold font) as shown in Figs 3-5. The monocultures were used to calibrate the model and the mixtures were used to validate the model. NPP = net primary productivity, W_S = stem mass, W_R= root mass. The statistical information includes the relative average error (e%), the relative mean absolute error (MAE%), the mean square error (MSE), the model efficiency (EF), the slope of the relationship forced through the origin, the *P*-value for the test of whether the slope of the relationship is significantly different from 1, and the R^2 values. Foliage growth and root growth are not considered due to the low reliability of calculating those variables using allometric equations.

Treatment	Species	Variable	e%	MAE%	MSE	EF	slope	P-value	R^2
Mixture	*F. sylvatica*	Basal area	17.3	20.4	17.99	0.39	0.84	< 0.0001	0.98
Mixture	*P. sylvestris*	Basal area	22.8	25.4	62.4	0.29	0.78	< 0.0001	0.98
Mixture	Mixture total	Basal area	20.5	20.7	125.72	0.12	0.81	< 0.0001	0.99
Monoculture	***F. sylvatica***	**Basal area**	**11.5**	**14.9**	**39.17**	**0.54**	**0.87**	**< 0.0001**	**0.99**
Monoculture	***P. sylvestris***	**Basal area**	**17.1**	**21.5**	**85.53**	**0.09**	**0.84**	**< 0.0001**	**0.98**
Mixture	*F. sylvatica*	Diameter	10.9	11.4	9.59	0.67	0.89	< 0.0001	0.99
Mixture	*P. sylvestris*	Diameter	11.4	12.2	23.6	0.83	0.89	< 0.0001	1
Monoculture	***F. sylvatica***	**Diameter**	**3.6**	**16.9**	**21.01**	**0.76**	**0.91**	**0.0009**	**0.97**
Monoculture	***P. sylvestris***	**Diameter**	**13.4**	**14.9**	**26.16**	**0.66**	**0.87**	**< 0.0001**	**0.99**
Mixture	*F. sylvatica*	Height	2.7	14.7	13.43	0.25	0.95	0.1598	0.97
Mixture	*P. sylvestris*	Height	5	15.7	20.51	0.03	0.94	0.0901	0.97
Monoculture	***F. sylvatica***	**Height**	**-7.2**	**22.2**	**31.74**	**-0.44**	**1.02**	**0.725**	**0.94**
Monoculture	***P. sylvestris***	**Height**	**2.7**	**13.4**	**15.29**	**0.5**	**0.98**	**0.4642**	**0.97**
Mixture	*F. sylvatica*	W_S	-12.7	16.4	1719.55	0.67	1.14	0.0017	0.97
Mixture	*P. sylvestris*	W_S	-8.9	15.1	968.68	0.84	1.11	0.0094	0.97
Mixture	Mixture total	W_S	-11.1	14.1	4513.11	0.74	1.13	0.0012	0.97
Monoculture	***F. sylvatica***	**W_S**	**-12.5**	**13.6**	**1962.85**	**0.94**	**1.12**	**< 0.0001**	**0.99**
Monoculture	***P. sylvestris***	**W_S**	**-7.3**	**13.2**	**802.2**	**0.9**	**1.07**	**0.0102**	**0.98**
Mixture	*F. sylvatica*	W_S growth	-28.6	50.2	14.79	-0.36	1.18	0.2776	0.68
Mixture	*P. sylvestris*	W_S growth	-35.8	60	8.56	-0.22	1.21	0.3436	0.55
Mixture	Mixture total	W_S growth	-31.2	45.8	36.81	-0.26	1.3	0.0796	0.71
Monoculture	***F. sylvatica***	**W_S growth**	**-43.4**	**53.1**	**24.49**	**0.23**	**1.57**	**0.0002**	**0.76**
Monoculture	***P. sylvestris***	**W_S growth**	**22.7**	**100.3**	**44.17**	**0.12**	**0.87**	**0.6387**	**0.25**
Mixture	*F. sylvatica*	Total biomass	-4.7	15.1	1796.76	0.71	1.05	0.2749	0.96
Mixture	*P. sylvestris*	Total biomass	-1.2	16.9	1430.82	0.82	1.03	0.5098	0.96
Mixture	Mixture total	Total biomass	-3.2	13	4819.96	0.77	1.04	0.2529	0.97
Monoculture	***F. sylvatica***	**Total biomass**	**-8.6**	**12.8**	**2155.51**	**0.95**	**1.09**	**< 0.0001**	**0.99**
Monoculture	***P. sylvestris***	**Total biomass**	**3.9**	**15**	**1150.63**	**0.9**	**0.96**	**0.1362**	**0.98**
Mixture	*F. sylvatica*	NPP	-18.5	49.1	16.56	-0.36	1.03	0.8551	0.68
Mixture	*P. sylvestris*	NPP	-27.7	65	12.38	-0.5	0.91	0.6374	0.47
Mixture	Mixture total	NPP	-22	43.2	41.9	-0.29	1.12	0.4352	0.7
Monoculture	***F. sylvatica***	**NPP**	**-42.6**	**55.9**	**30.74**	**0.17**	**1.49**	**0.002**	**0.72**
Monoculture	***P. sylvestris***	**NPP**	**49.7**	**104.9**	**60.03**	**0.09**	**0.71**	**0.1695**	**0.27**
Mixture	*F. sylvatica*	RP - Basal area	17.3	20.4	17.99	0.39	0.84	< 0.0001	0.98
Mixture	*P. sylvestris*	RP - Basal area	22.8	25.4	62.4	0.29	0.78	< 0.0001	0.98
Mixture	Mixture total	RP - Basal area	20.5	20.7	125.72	0.12	0.81	< 0.0001	0.99
Mixture	*F. sylvatica*	RP - diameter	5.4	11.2	0.17	0.71	0.94	0.058	0.98
Mixture	*P. sylvestris*	RP - diameter	-0.3	5.2	0.02	0.95	1	0.9049	1

Mixture	*F. sylvatica*	RP - height	19.2	23.1	0.69	-0.45	0.79	< 0.0001	0.94
Mixture	*P. sylvestris*	RP - height	-2.1	12.1	0.14	0.69	1.03	0.4353	0.97
Mixture	*F. sylvatica*	RP - W_R	27.8	31.5	0.19	-0.92	0.78	< 0.0001	0.96
Mixture	*P. sylvestris*	RP - W_R	-12.1	20.8	0.13	0.26	1.15	0.0251	0.93
Mixture	Mixture total	RP - W_R	3.8	13	0.04	0.52	0.97	0.3788	0.97
Mixture	*F. sylvatica*	RP - W_S growth	28.4	50.2	0.83	-0.54	0.75	0.0025	0.81
Mixture	*P. sylvestris*	RP - W_S growth	-34.5	57.3	1.68	-0.29	1.35	0.2047	0.51
Mixture	Mixture total	RP - W_S growth	10.3	43.6	0.64	-0.06	0.89	0.3024	0.73
Mixture	*F. sylvatica*	RP - W_S	1.8	10.9	0.04	0.87	0.99	0.6051	0.98
Mixture	*P. sylvestris*	RP - W_S	-4.1	13.2	0.05	0.85	1.07	0.0393	0.98
Mixture	Mixture total	RP - W_S	-2.4	8.6	0.03	0.88	1.04	0.1027	0.99
Mixture	*F. sylvatica*	RP - Total biomass	4.7	11.8	0.05	0.83	0.96	0.1527	0.98
Mixture	*P. sylvestris*	RP - Total biomass	-6.5	13.6	0.06	0.78	1.1	0.0085	0.98
Mixture	Mixture total	RP - Total biomass	-1.8	8.8	0.03	0.85	1.04	0.1768	0.99

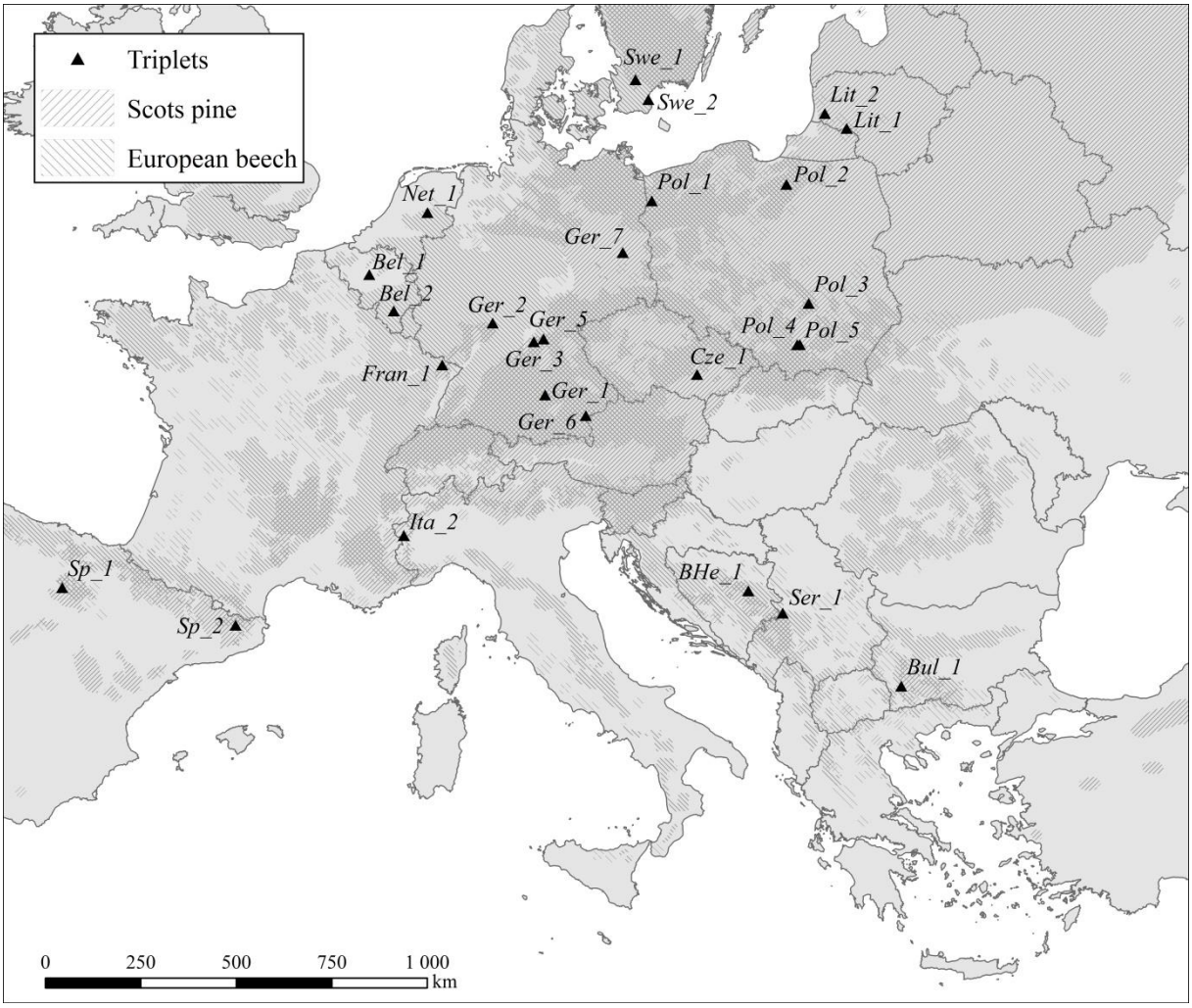

Figure 1. The locations of the 26 sites with plots of *Pinus sylvestris* and *Fagus sylvatica* in relation to their current distributions according to EUFORGEN (http://www.euforgen.org/distribution-maps/).

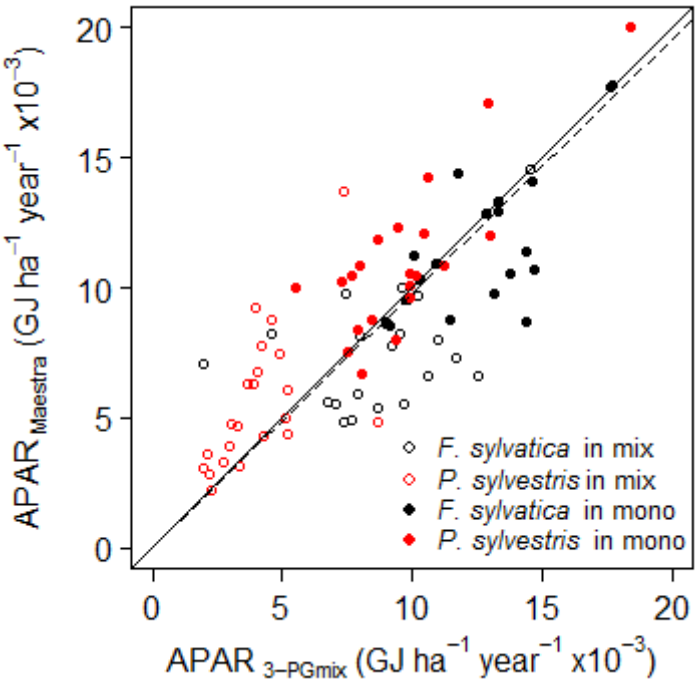

Figure 2. Comparison of predicted absorption of photosynthetically active radiation by Maestra ($APAR_{Maestra}$) and 3-PG_{mix} ($APAR_{3\text{-}PGmix}$) for the year 2014. The solid line is a 1:1 line and the dashed line is fitted to the data that passes through the origin.

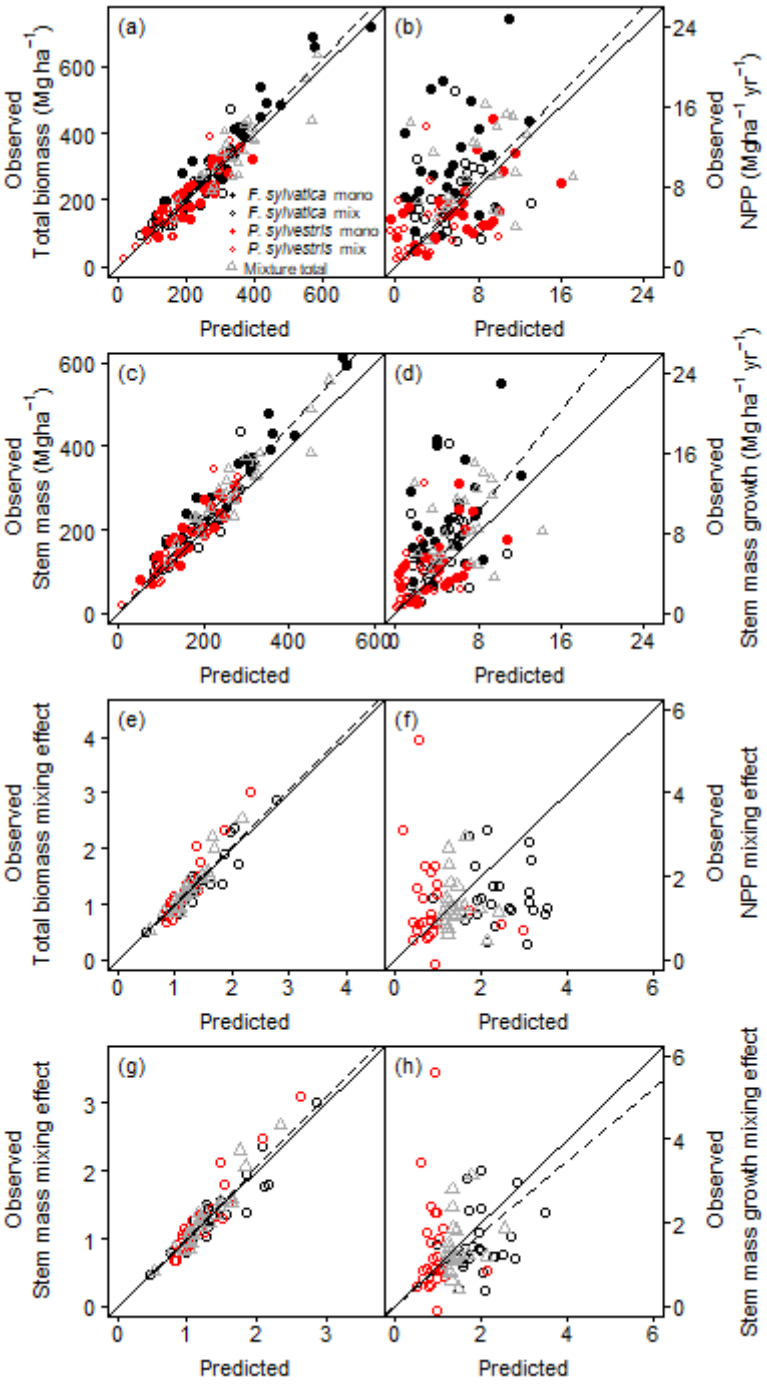

Figure 3. Comparison of observed and predicted total biomass (TB, a), net primary productivity (NPP, b), stand stem mass (W_S, c), stem mass growth (d), the mixing effects, in terms of relative productivity (RP, Equations 1 and 2) for total biomass (TB, e), net primary productivity (NPP, f), stand stem mass (W_S, g) and stem mass growth (h). Growth is for the year 2012 and stocks are for the end of 2012. The solid lines are 1:1 lines and the dashed lines are lines fitted to the data that pass through the origin. For each species-treatment combination n=26.

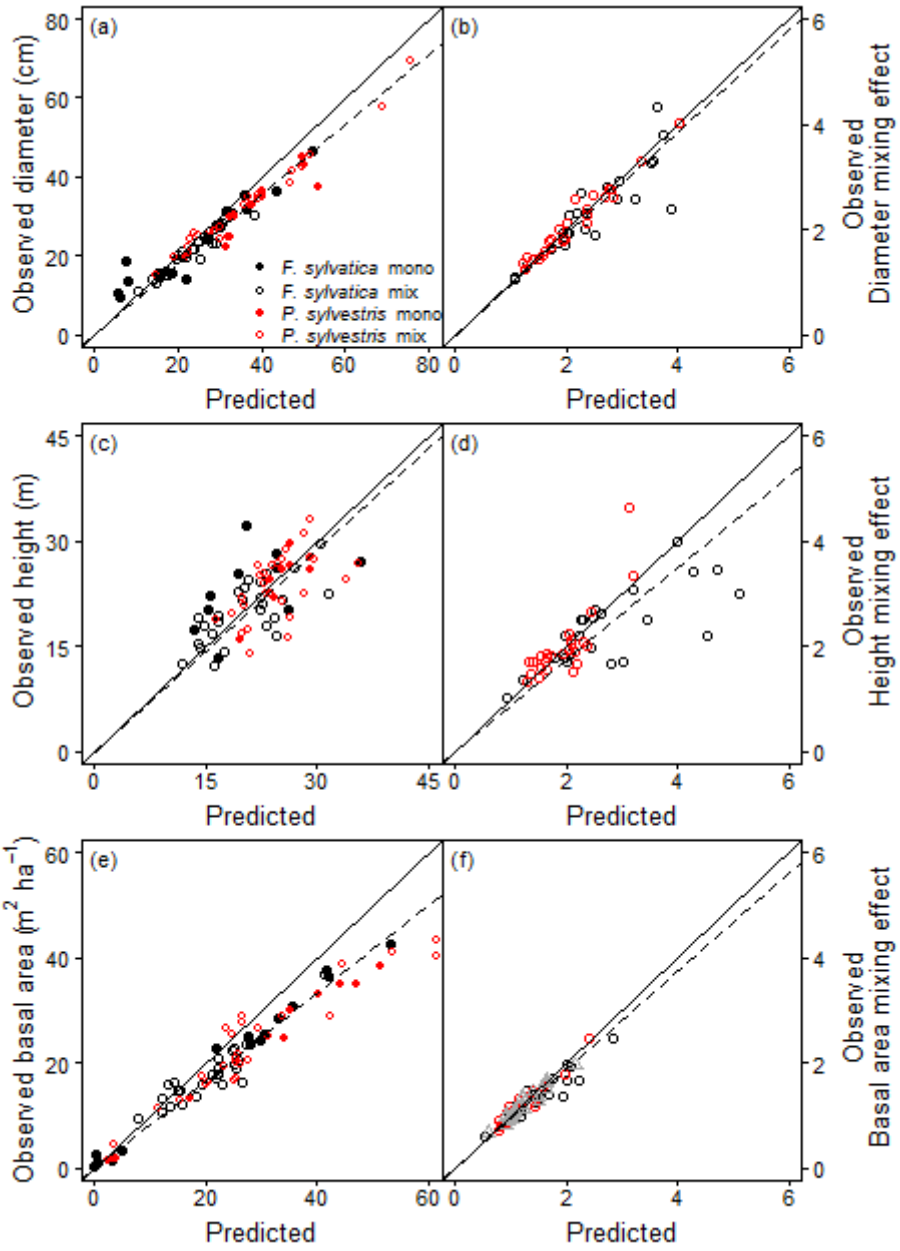

Figure 4. Comparison of observed and predicted diameter at 1.3 m (*B*, a), the mixing effect in terms of relative productivity (RP) of diameter (b), height (c), RP of height (d), basal area (e) and RP of basal area (f). All data is for the end of 2012. The solid lines are 1:1 lines and the dashed lines are lines fitted to the data that pass through the origin. For each species-treatment combination n=26.

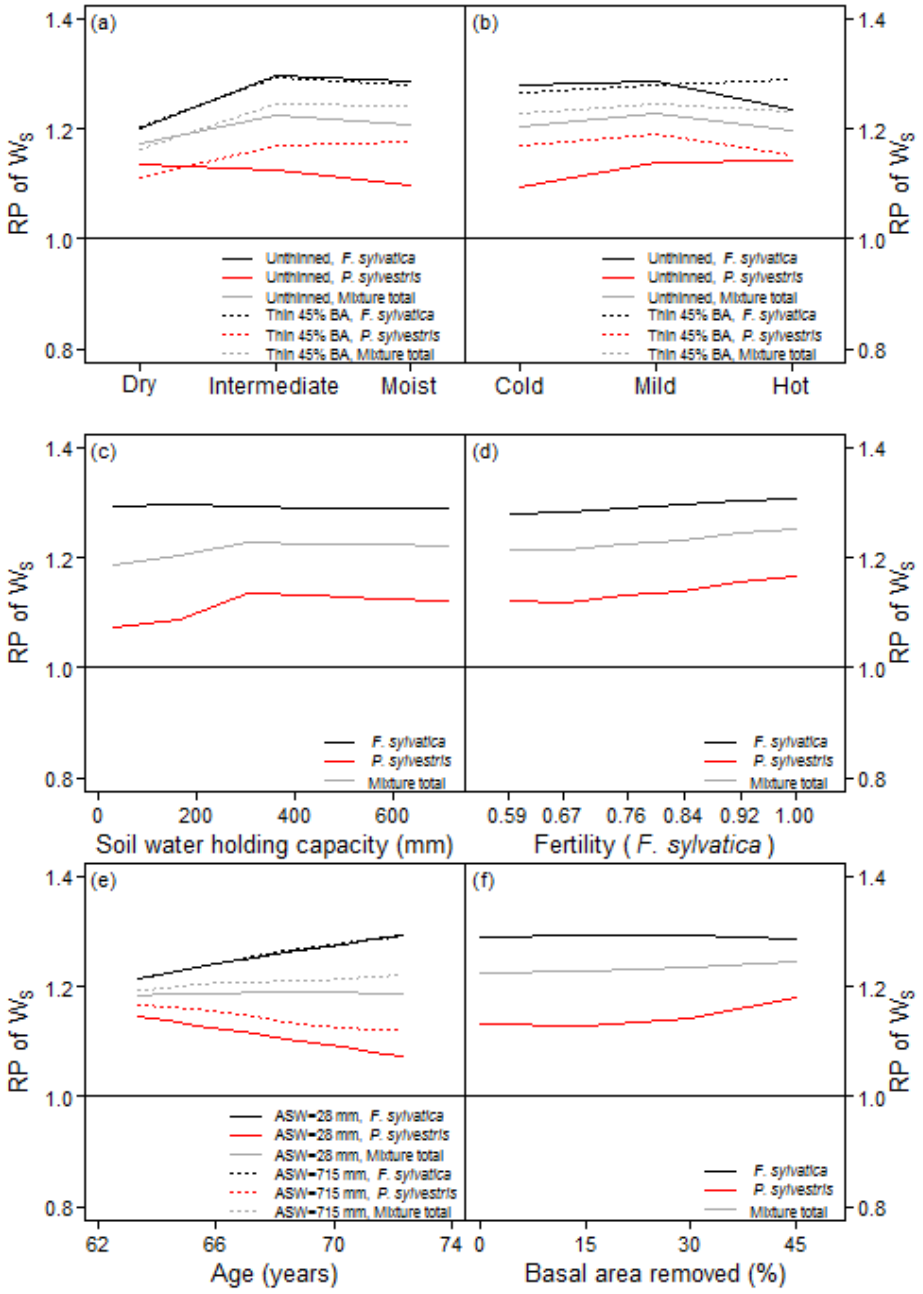

Figure 5. The simulated mixing effect, in terms of the relative productivity (RP, Equations 1 & 2) calculated using stem mass (W_S) along gradients in terms of precipitation (a), temperature (b), soil water holding capacity (c), soil fertility (d), age (e) and thinning intensity (f). The levels of each gradient are described in the text. If RP is >1 then the W_S was greater in mixture than monoculture, whereas if RP is <1 the W_S was lower in the mixture than in monoculture. Except for (e), all patterns are only shown for the final year of the simulation (2013). Soil fertility (FR) for both species were linearly correlated so only *F. sylvatica* is shown on the x-axis in (d). ASW indicates the available soil water holding capacity for the simulated site.

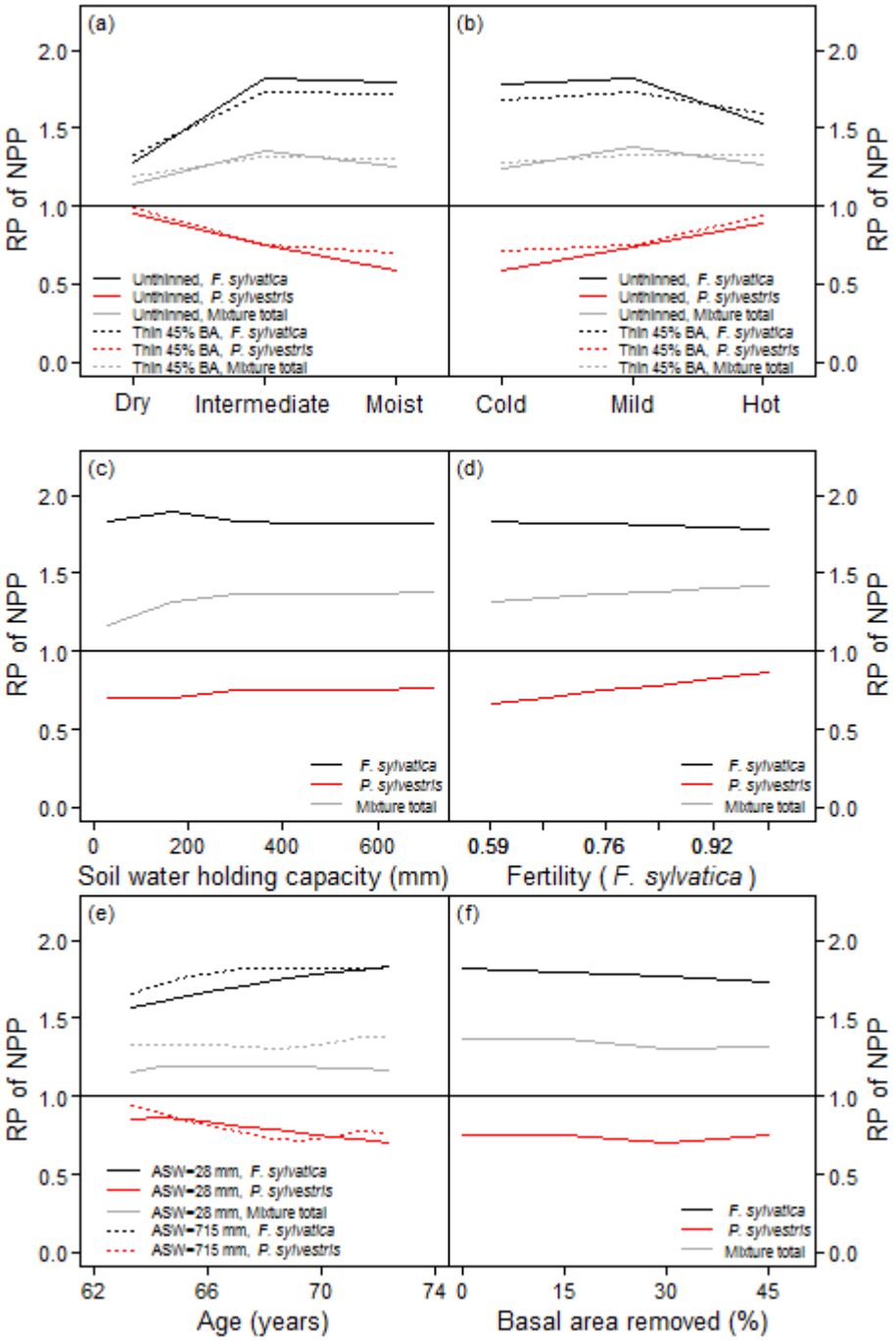

Figure 6. The simulated mixing effect, in terms of the relative productivity (RP, Equations 1 & 2) calculated using NPP along gradients in terms of precipitation (a), temperature (b), potential available soil water (c), soil fertility (d), age (e) and thinning intensity (f). The levels of each gradient are described in the text. If RP is >1 then the NPP was greater in mixture than monoculture, whereas if RP is <1 the NPP was lower in the mixture than in monoculture. Except for (e), all patterns are only shown for the final year of the simulation (2013). Soil fertility (FR) for both species were linearly correlated so only *F. sylvatica* is shown on the x-axis in (d). ASW indicates the available soil water holding capacity for the simulated site.

Appendix A

Table A1. Description of parameters, their values and sources. Source refers to "Default" values for *Eucalyptus globulus* in 3-PG$_{PJS}$ 2.7, "Observed" values measured in this study or obtained from published observations, and "Fitted" values that were obtained, as described in the text. Sources for published observations are described in the methodology section.

Parameter	Symbol	Units	Source	*Pinus sylvestris*	*Fagus sylvatica*
Biomass partitioning and turnover					
Allometric relationships & partitioning					
Foliage:stem partitioning ratio @ *B*=2 cm	p_2	-	Fitted	0.70	0.70
Foliage:stem partitioning ratio @ *B*=20 cm	p_{20}	-	Fitted	0.21	0.06
Constant in the stem mass v. *B* relationship	a_S	-	Observed	0.126	0.183
Power in the stem mass v. *B* relationship	n_S	-	Observed	2.268	2.390
Maximum fraction of NPP to roots	η_{Rx}	-	Fitted	0.7	0.7
Minimum fraction of NPP to roots	η_{Rn}	-	Fitted	0.3	0.3
Litterfall & root turnover					
Maximum litterfall rate	γ_{Fx}	1/month	Fitted	0.015	0.02
Litterfall rate at t = 0	γ_{F0}	1/month	Default	0.001	0.001
Age at which litterfall rate has median value	$t_{\gamma F}$	months	Observed	60	60
Average monthly root turnover rate	γ_R	1/month	Fitted	0.004	0.015
If deciduous, the month when leaves produced	$leaf_P$	month	Observed	0	4
If deciduous, the month when leaves fall	$leaf_L$	month	Observed	0	11
NPP & conductance modifiers					
Temperature modifier (f_T)					
Minimum temperature for growth	T_{min}	deg. C	Observed	-5	-5
Optimum temperature for growth	T_{opt}	deg. C	Observed	15	20
Maximum temperature for growth	T_{max}	deg. C	Observed	35	25
Frost modifier (f_F)					
Days production lost per frost day	k_F	days	Default	1	1
Fertility effects					
Value of 'm' when FR = 0	m_0	-	Default	0	0
Value of 'f_N' when FR = 0	f_{N0}	-	Fitted	0.2	0.5
Power of (1-FR) in 'f_N'	n_{fN}	-	Default	1	1
Age modifier (f_{AGE})					
Maximum stand age used in age modifier	t_x	years	Observed	350	300
Power of relative age in function for f_{AGE}	n_{age}	-	Default	4	4
Relative age to give f_{AGE} = 0.5	r_{age}	-	Default	0.95	0.95
Canopy structure and processes					
Specific leaf area					
Specific leaf area at age 0	σ_0	m^2/kg	Observed	4.29	24.7
Specific leaf area for mature leaves	σ_1	m^2/kg	Observed	4.29	19.4
Age at which specific leaf area = (SLA0+SLA1)/2	t_σ	years	Observed	1	35
Light interception					
Extinction coefficient for absorption of PAR by canopy	k or k_H	-	Observed	0.38	0.42
Age at canopy closure	t_c	years	Observed	10	10
Maximum proportion of rainfall evaporated from canopy	I_{Rx}	-	Observed	0.395	0.237
LAI for maximum rainfall interception	L_{Ix}	-	Default	3	3
LAI for 50% reduction of VPD in canopy	L_{50D}	-	Default	5	5
Production and respiration					
Canopy quantum efficiency	α_{Cx}	molC/molPAR	Observed	0.049	0.050
Ratio NPP/GPP	Y	-	Default	0.47	0.47
Conductance					
Minimum canopy conductance	g_{Cmin}	m/s	Default	0	0
Maximum canopy conductance	g_{Cmax}	m/s	Default	0.02	0.02
LAI for maximum canopy conductance	L_{gCmax}	-	Default	3.33	3.33
Defines stomatal response to VPD	k_D	1/mBar	Default/observed	0.05	0.057
Canopy boundary layer conductance	g_B	m/s	Default	0.2	0.2
Basic Density					
Minimum basic density - for young trees	ρ_0	t/m3	Observed	0.395	0.567
Maximum basic density - for older trees	ρ_1	t/m3	Observed	0.395	0.567
Age at which $\rho = (\rho_0 + \rho_1)/2$	t_ρ	years	Not applicable	1	1
Stem height					
Constant in the stem height relationship	a_H	-	Observed	4.589	1.008
Power of *B* in the stem height relationship	n_{HB}	-	Observed	0.474	0.450
Power of competition in the stem height relationship	n_{HC}	-	Observed	0	0
Crown shape					
Crown shape (1=cone, 2=ellipsoid, 3=half-ellipsoid, 4=rectangular)	-	-	Default	3	3
Crown diameter					
Constant in the crown diameter relationship	a_K	-	Observed	1.376	0.939
Power of B in the crown diameter relationship	n_{KB}	-	Observed	0.554	0.581
Power of height in the crown diameter relationship	n_{KH}	-	Observed	0	0
Power of competition in the crown diameter relationship	n_{KC}	-	Observed	-0.266	0

Power of relative height in the crown diameter relationship	n_{Krh}	-	Observed	0	0
Live-crown length					
Constant in the LCL relationship	a_{HL}	-	Observed	2.189	6.269
Power of *B* in the LCL relationship	n_{HLB}	-	Observed	0.563	0.189
Power of LAI in the LCL relationship	n_{HLL}	-	Observed	0	0
Power of competition in the LCL relationship	n_{HLC}		Observed	-0.262	0
Power of relative height in the LCL relationship	n_{HLrh}		Observed	0.678	0.655
Diameter distributions					
Constant for Weibull scale parameter of *B* dist.	sc_{B0}	-	Observed	0.278	0.194
Slope of DBH in relationship for Weibull scale parameter	sc_{BB}		Observed	1.152	1.225
Slope of relative height for Weibull scale parameter	sc_{Brh}		Observed	0	0
Slope of age in relationship for Weibull scale parameter	sc_{Bt}		Observed	0	0.128
Slope of competition for Weibull scale parameter	sc_{BC}		Observed	0.054	0
Constant in the relationship for Weibull shape parameter	sh_{B0}		Observed	1.228	0.788
Slope of DBH in relationship for Weibull shape parameter	sh_{BB}		Observed	0	0.316
Slope of relative height for Weibull shape parameter	sh_{Brh}		Observed	1.189	1.614
Slope of age in relationship for Weibull shape parameter	sh_{Bt}		Observed	0	0
Slope of competition for Weibull shape parameter	sh_{BC}		Observed	0.214	-0.117
Constant in the relationship for Weibull location parameter	loc_{B0}		Observed	0.987	1.636
Slope of DBH in relationship for Weibull location parameter	loc_{BB}	-	Observed	0.872	0.505
Slope of relative height for Weibull location parameter	loc_{Brh}	-	Observed	0.023	-0.626
Slope of age in relationship for Weibull location parameter	loc_{Bt}	-	Observed	0	0
Slope of competition for Weibull location parameter	loc_{BC}	-	Observed	-0.106	0.046
ws distributions					
Constant for Weibull scale parameter of *ws* dist.	sc_{w0}		Observed	0.090	0.022
Slope of DBH in relationship for Weibull scale parameter	sc_{wB}		Observed	2.084	2.605
Slope of relative height for Weibull scale parameter	sc_{wrh}		Observed	0	-1.815
Slope of age in relationship for Weibull scale parameter	sc_{wt}		Observed	0.271	0.321
Slope of competition for Weibull scale parameter	sc_{wC}		Observed	-0.122	0.090
Constant in the relationship for Weibull shape parameter	sh_{w0}		Observed	1.134	0.646
Slope of DBH in relationship for Weibull shape parameter	sh_{wB}		Observed	0	0.269
Slope of relative height for Weibull shape parameter	sh_{wrh}		Observed	0.945	1.740
Slope of age in relationship for Weibull shape parameter	sh_{wt}		Observed	0	0
Slope of competition for Weibull shape parameter	sh_{wC}		Observed	0.122	-0.143
Constant in the relationship for Weibull location parameter	loc_{w0}		Observed	0.228	0.143
Slope of DBH in relationship for Weibull location parameter	loc_{wB}	-	Observed	2.204	1.028
Slope of relative height for Weibull location parameter	loc_{wrh}	-	Observed	0	-3.450
Slope of age in relationship for Weibull location parameter	loc_{wt}	-	Observed	-0.418	0.453
Slope of competition for Weibull location parameter	loc_{wC}	-	Observed	0	0.208
Conversion factors					
Intercept of net v. solar radiation relationship	Q_a	W/m2	Default	-90	-90
Slope of net v. solar radiation relationship	Q_b	-	Default	0.8	0.8
Molecular weight of dry matter		gDM/mol	Default	24	24
Conversion of solar radiation to PAR		mol/MJ	Default	2.3	2.3
Calculation options					
Apply 3PGpjs light model = no					
Apply 3PGpjs water balance = no					
Apply 3PGpjs Physmod = yes					
Dbh and ws distribution type = provided					

Table A2. Stand and site characteristics for the 26 sites sorted by the de Martonne aridity index. When a given characteristic varied between plots within a site, values for each plot are provided as *F. sylvatica* monoculture / *P. sylvestris* monoculture / Mixture. Site index is a site productivity index calculated as the height of the 100 largest-diameter trees per ha at age 50 years (using data from monocultures only).

ID	Site code	Longitude	Latitude	Altitude	Aspect (°)	Slope (°)	Mean annual temperature (°C)	Mean annual precipitation (mm)	Substrate	de Martonne index	Site index	Date leaves begin absorbing PAR	Date leaves stop absorbing PAR
Ger_7	1061	13°36'58"/57"/54"	52°04'43"/43"/45"	76/68/76	0	0	8.6	520	sandy	28	16.9/13.1	05/05/2013	15/11/2013
Pol_1	1035	14°36'18"	53°20'7"	60	0	0	9.2	556	loamy sand and sand	29	27.3/26.9	30/04/2013	31/10/2013
Ger_6	1070	12°44'08"	48°11'12"	40	0	0	8	560	slightly loamy sand	31.1	15.8/12.8	30/04/2013	15/10/2013
Ger_5	1034	08°10'49"	48°59'12"	370	0	3	10	675	slightly loamy sand	33.4	24.4/23.6	30/04/2013	22/10/2013
Cze_1	1049	16°36'10"/7"/9"	49°18'14"/15"/14"	435/445/440	45	5-15/0-10/5-10	7.5	620	cambisol mezotrofic	35.4	23.8/23.0	25/04/2013	22/10/2013
Pol_4	1044	20°24'33"/23'38"/13'46"	50°0'51"/2'53"/1'28"	210/205/210	0	0 / 0 / 4	8.2	650	slightly loamy sand	35.7	15.8/21.3	07/05/2013	15/11/2013
Pol_5	1045	20°14'21"/20'50"/19'37"	50°1'30"/2'31"/1'36"	210/210/220	0	0	8.2	650	loamy sand	35.7	25.8/24.5	07/05/2013	15/11/2013
Ger_3	1032	10°58'13''	49°53'12''	250	30	2	8	650	loamy sand	36.1	24.4/25.2	22/04/2013	31/10/2013
Pol_2	1036	19°54'42"	53°48'19"	136	0	0	7.9	666	slightly loamy sand	37.2	19.1/25.5	07/05/2013	31/10/2013
Pol_3	1037	20°41'09"	50°59'28"	383	275	2	7.8	662	sandstone loamy sand and loam	37.2	22.6/20.5	30/04/2013	31/10/2013
Ger_1	1033	11°14'12"	48°34'58"	430	45	1	8.5	700	slightly loamy sand	37.8	27.6/22.7	30/04/2013	22/10/2013
Ger_2	1031	9°3'54"	50°6'49"	250	20	0	9	720	slightly loamy sand	37.9	23.1/25.7	15/04/2013	22/10/2013
Swe_1	1054	13°35'29"/11"/35"	56°8'50"/8'59"/9'12"	130/120/110	270/270/125	10/11/2017	8	700	loamy sand	38.9	13.3/21.0	22/04/2013	15/10/2013
Bel_1	1063	04°19'30"	50°45'06"	120	0	0	10.5	852	loam	41.6	12.0/10.9	01/05/2013	31/10/2013
Net_1	1043	6°1'22"/28"/20"	52°25'40"/41"/41"	34/34/35	90/0/45	3.4/0/2.3	9.7	825	coarse sand	41.9	17.4/17.9	01/05/2013	01/11/2013
Lit_1	1051	22°24'24"	55°04'47.30"	20	0	0	6.5	750	sand and slightly loamy sand	45.5	22.3/19.5	05/05/2013	15/10/2013
Sp_1	1042	3°10'33''W/0''W/19''W	42°6'10''/ 5'48''/5'57''	1252/1339/1289	45/0/315	43/53/45	8.9	860	sandy loam	45.5	24.8/20.9	15/05/2013	15/11/2013
Bul_1	1047	23°21'02''	41°53'44''	1180	360/360/330	20/20/15	6	750	loamy sand	46.9	25.9/25.1	31/05/2013	01/11/2013
Swe_2	1053	14°11'49"/51"/46"	55°42'41"/42"/33"	20/25/30	180/180/0	15/05/2004	7	800	sandy till	47.1	22.0/22.0	22/04/2013	15/10/2013
Fran_1	1040	7°29'14''	48°58'42''	275	315	28/38/35	9.7	948	sandstone sandy soil	48.1	22.2/23.0	15/05/2013	15/11/2013
BHe_1	1059	18°29'56"	44°13'35"	627	225	25	9.5	939	loam to sandy clay	48.2	13.2/16.1	30/04/2013	01/11/2013
Lit_2	1052	21°32'23"	55°27'02"	25	0	0	6.5	800	sand and slightly loamy sand	48.5	13.6/22.9	05/05/2013	15/10/2013
Ita_2	1062	07°03'53"	44°54'12"	1250	315	25	7.9	938	sandy loam	52.4	19.9/16.9	30/04/2013	01/11/2013
Ser_1	1056	19°37'30"	43°42'17"	1090	0	20	7.7	1020	loam	57.6	11.7/14.7	30/04/2013	01/11/2013
Sp_2	1041	2°16'0"/16'26"/15'44"	42°10'15"/46"/18"	1065/1209/1074	45/315/45	39.8/24.4/26.6	8	1100	loam slightly clay	61.1	24.3/9.5	15/05/2013	15/11/2013
Bel_2	1057	05°27'00"	50°01'48"	530	180	8	7.5	1175	stony loam	67.1	13.2/17.3	01/05/2013	15/10/2013

Appendix B

Height, live-crown length and crown diameter equations (Equations 3-5)

The height of each species was a function of diameter, but for *F. sylvatica*, the competition index was also a significant predictor (Table B1). The crown diameter of *P. sylvestris* was also related to the competition index, in addition to stem diameter, while the crown diameter of *F. sylvatica* was only significantly related by stem diameter. Live-crown lengths of both species were related to the competition index and *P. sylvestris* crown lengths were also related to their relative height (Table B1).

Table B1. Parameter estimates (with their standard errors) and random effects for Equations 3 to 5 that describe the (ln-transformed) height (m), crown diameter (m) and live-crown length (m) of *P. sylvestris* and *F. sylvatica*.

	Stem height	
	F. sylvatica	*P. sylvestris*
$\ln(a_H)$	-0.002 (0.215)	1.519 (0.054)
n_{HB}	0.538 (0.008)	0.474 (0.011)
n_{HC}	0.45 (0.071)	
Correction factor	1.0095	1.0047
n	2324	1778
ε_{ij}	0.158	0.118
Standard deviation (sd) for random effects (sd_i / sd_{ij})		
Estimate	0.137 / 0.161	0.177 / 0.088
Lower	0.083 / 0.122	0.125 / 0.065
Upper	0.228 / 0.213	0.252 / 0.118

	Live-crown length	
	F. sylvatica	*P. sylvestris*
$\ln(a_{HL})$	1.802 (0.091)	0.753 (0.322)
n_{HLB}	0.189 (0.024)	0.563 (0.036)
n_{HLC}	0.655 (0.037)	-0.266 (0.101)
n_{HLrh}		0.678 (0.055)
Correction factor	1.0344	1.0304
n	2314	1778
ε_{ij}	0.286	0.278
Standard deviation (sd) for random effects (sd_i / sd_{ij})		
Estimate	0.226 / 0.146	0.164 / 0.132
Lower	0.156 / 0.107	0.102 / 0.093
Upper	0.328 / 0.198	0.264 / 0.188

	Crown diameter	
	F. sylvatica	*P. sylvestris*
$\ln(a_K)$	-0.093 (0.059)	0.283 (0.28)

n_{KB}	0.581 (0.015)	0.554 (0.022)
n_{KH}		
n_{KC}		-0.277 (0.091)
Correction factor	1.0303	1.0376
n	2108	1571
ε_{ij}	0.279	0.283
Standard deviation (sd) for random effects (sd_i / sd_{ij})		
Estimate	0.125 / 0.202	0.128 / 0.104
Lower	0.056 / 0.148	0.08 / 0.071
Upper	0.277 / 0.277	0.205 / 0.154

n=the sample number; ε_{ij} = the residual variance, correction factor is as described in the text (Snowden, 1991).

Diameter and stem mass distributions

3-PG_{mix} uses diameter or stem mass distributions for two main purposes. One is to correct for the bias that can result from Jensen's Inequality when allometric equations are used to calculate means of variables (e.g. mean diameter) instead of individual tree values; the mean of a function is not the same as the function of the mean (Duursma and Robinson, 2003). The second use of the distributions, is to provide the user with the option to thin the stand and to obtain outputs for a given number of crop trees (e.g. the largest 100 trees per ha) or the parameters of the Weibull distributions themselves (Forrester and Tang, 2016).

In this study, the distributions were described using 3-parameter Weibull distributions (Forrester and Tang, 2016). The scale, shape and location parameters of the Weibull distributions were calculated using the percentile method, as described by Nanang (1998) using the data collected from the triplets. The w_s was calculated using generalised biomass equations from Forrester *et al.* (2017b). In the mixed-species plots, the size distributions of a given species were converted to equivalent monospecific size distributions by dividing the trees per ha of each size class (for the given species) by the mixing proportion for that species in terms of basal area.

The scale, shape and location parameters were then fitted to Equations B1 to B6 where they are described as functions of mean diameter (B, cm), relative height (rh, height of the target species divided by the mean height of all species in the plot), age (A, years) and competition, which as calculated using Equation 6. Equations B1 to B6 were fitted as mixed models with site as the random variable using the *nlme* package for fitting the mixed models (Harrison *et al.*, 2009) with R 3.2.1 (R Core Team, 2015).

$$\ln(loc_B) = \mathrm{loc_{B0}} + \mathrm{loc_{BB}} \times ln(B) + \mathrm{loc_{Brh}} \times ln(rh) + \mathrm{loc_{Bt}} \times ln(Age) + \mathrm{loc_{BC}} \times ln(C) \quad \text{(B1)}$$

$$ln(sc_B) = sc_{B0} + sc_{BB} \times ln(B) + sc_{Brh} \times ln(rh) + sc_{Bt} \times ln(Age) + sc_{BC} \times ln(C) \quad \text{(B2)}$$

$$ln(sh_B) = sh_{B0} + sh_{BB} \times ln(B) + sh_{Brh} \times ln(rh) + sh_{Bt} \times ln(Age) + sh_{BC} \times ln(C) \quad \text{(B3)}$$

$$ln(loc_w) = loc_{w0} + loc_{wB} \times ln(B) + loc_{wrh} \times ln(rh) + loc_{wt} \times ln(Age) + loc_{wC} \times ln(C) \quad \text{(B4)}$$

$$ln(sc_w) = sc_{w0} + sc_{wB} \times ln(B) + sc_{wrh} \times ln(rh) + sc_{wt} \times ln(Age) + sc_{wC} \times ln(C) \quad \text{(B5)}$$

$$ln(sh_w) = sh_{w0} + sh_{wB} \times ln(B) + sh_{wrh} \times ln(rh) + sh_{wt} \times ln(Age) + sh_{wC} \times ln(C) \quad \text{(B6)}$$

where loc_{Bx}, sc_{Bx} and sh_{Bx} are fitted parameters for the B distributions, and loc_{wx}, sc_{wx} and sh_{wx} are fitted parameters for the w_s distributions.

Equations B1 to B6 differ from the equations in the original 3-PG$_{mix}$ described by Forrester and Tang (2016) because ln-transformations were found to be necessary to reduce heteroscedasticity and to linearize relationships. The parameter estimates for Equations B1 to B6 are shown in Table B2 and the distributions are shown in Figs B1 & B2.

Mean stand diameter, for the given species, was the strongest predictor of the shape of diameter distributions and also of the w_S distributions (Figs B1 and B2; Table B2). For both species, there were also small, but significant, effects of the competition index, relative height and age, with the exception of age in the *P. sylvestris* diameter distribution equations.

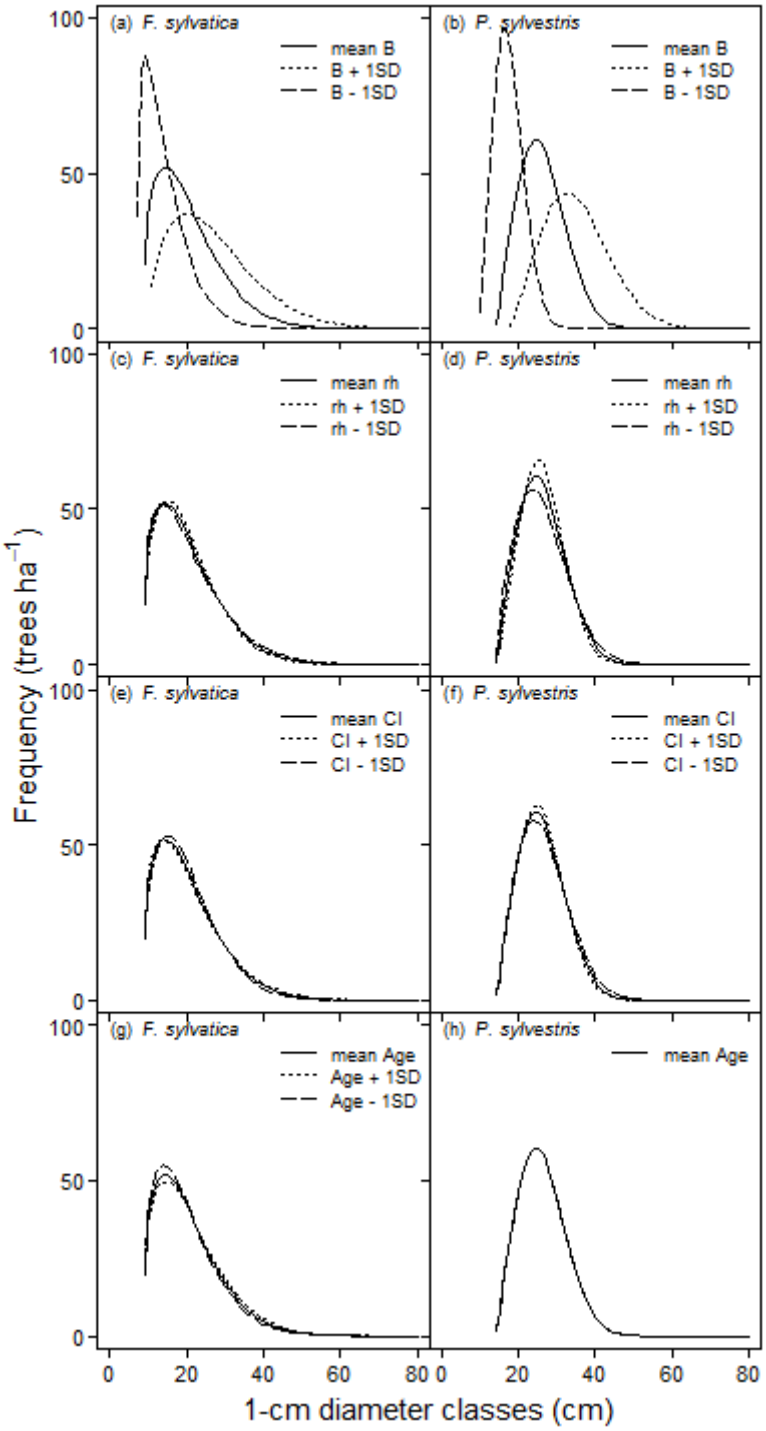

Figure B1. The effects of mean diameter (*B*), relative height (*rh*), age and competition index (*CI*; Equation 6) on the diameter distributions of *F. sylvatica* and *P. sylvestris*. These plots are created using Equations B1 to B6 and by varying only one of the independent variables at a time, and holding all others at their mean values for the given species.

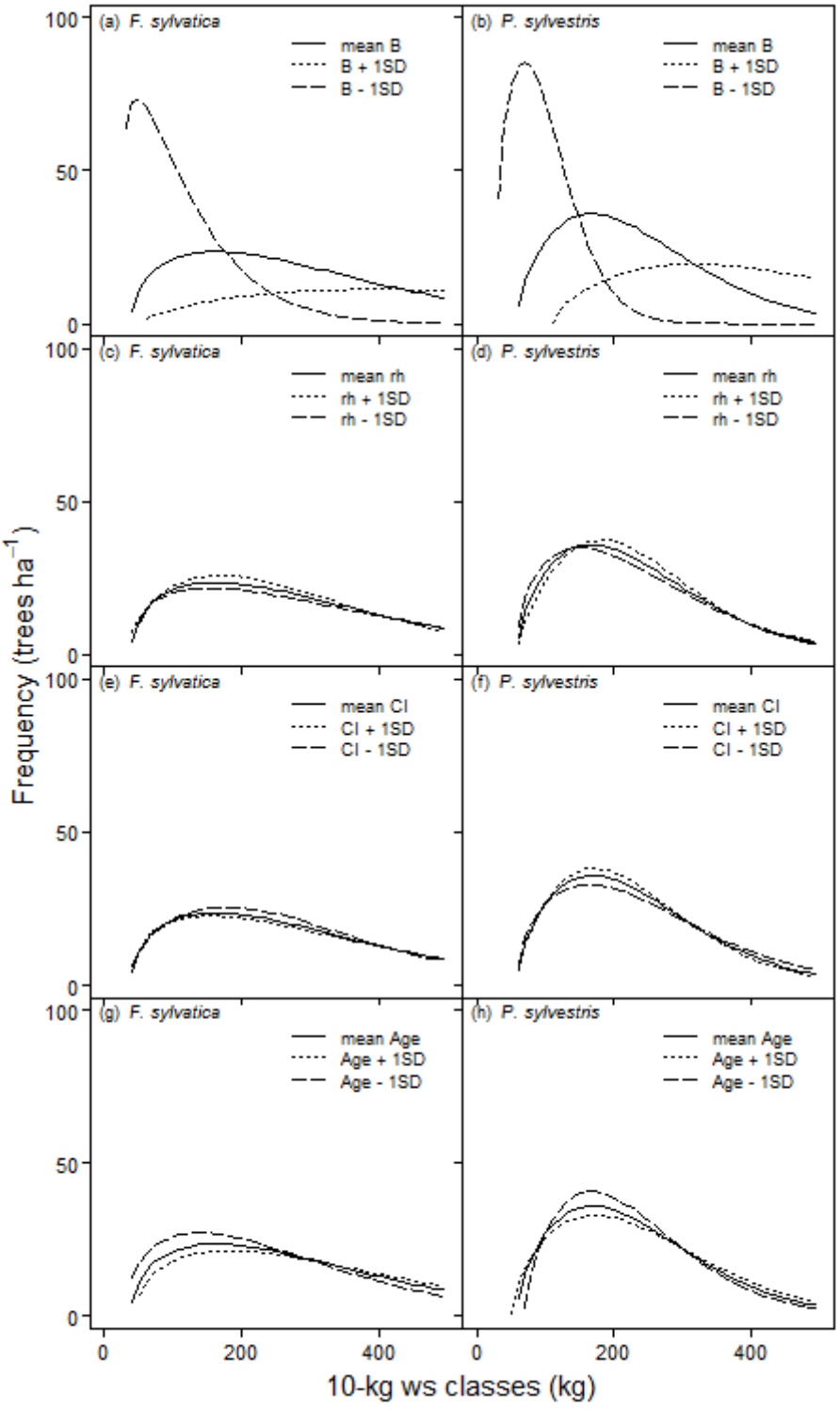

Figure B2. The effects of mean diameter (*B*), relative height (*rh*), age and competition index (*CI*; Equation 6) on the stem mass (w_s) distributions of *F. sylvatica* and *P. sylvestris*. These

plots are created using Equations B1 to B6 and by varying only one of the independent variables at a time, and holding all others at their mean values for the given species.

Table B2. Parameter estimates (with their standard errors) and random effects for Equations B1 to B6 that describe the (ln-transformed) parameters of Weibull distributions, for diameter and stem mass, of *P. sylvestris* and *F. sylvatica*. The parameters loc_{Bx}, sc_{Bx} and sh_{Bx} are fitted parameters for the diameter distributions and loc_{wx}, sc_{wx} and sh_{wx} are fitted parameters for the stem mass distributions.

Diameter distribution			**Stem mass distribution**		
Scale parameter					
	F.sylvatica	*P. sylvestris*		*F.sylvatica*	*P. sylvestris*
$ln(sc_{B0})$	-1.638 (0.202)	-1.28 (0.234)	$ln(sc_{w0})$	-3.812 (0.229)	-2.408 (0.306)
sc_{BB}	1.225 (0.031)	1.152 (0.06)	sc_{wB}	2.605 (0.042)	2.084 (0.052)
sc_{Brh}			sc_{wrh}	-1.815 (0.184)	
sc_{Bt}	0.128 (0.052)		sc_{wt}	0.321 (0.061)	0.271 (0.086)
sc_{BC}		0.054 (0.024)	sc_{wC}	0.09 (0.021)	-0.122 (0.021)
n	635	631	n	635	607
ε_i	0.089	0.193	ε_i	0.113	0.144
Standard deviation for random effects			*Standard deviation for random effects*		
Estimate	0.184	0.227	Estimate	0.147	0.213
Lower	0.139	0.227	Lower	0.107	0.16
Upper	0.244	0.404	Upper	0.201	0.284
Shape parameter					
	F.sylvatica	*P. sylvestris*		*F.sylvatica*	*P. sylvestris*
$ln(sh_{B0})$	-0.238 (0.179)	0.206 (0.115)	$ln(sh_{w0})$	-0.437 (0.207)	0.126 (0.112)
sh_{BB}	0.316 (0.059)		sh_{wB}	0.269 (0.068)	
sh_{Brh}	1.614 (0.291)	1.189 (0.193)	sh_{wrh}	1.74 (0.346)	0.945 (0.188)
sh_{Bt}			sh_{wt}		
sh_{BC}	-0.117 (0.032)	0.214 (0.04)	sh_{wC}	-0.143 (0.038)	0.122 (0.04)
n	635	631	n	635	607
ε_i	0.183	0.258	ε_i	0.221	0.25
Standard deviation for random effects			*Standard deviation for random effects*		
Estimate	0.156	0.267	Estimate	0.161	0.251
Lower	0.116	0.2	Lower	0.119	0.188
Upper	0.211	0.357	Upper	0.217	0.335
Location parameter					
	F.sylvatica	*P. sylvestris*		*F.sylvatica*	*P. sylvestris*
$ln(loc_{B0})$	0.492 (0.1)	-0.013 (0.225)	$ln(loc_{w0})$	-1.947 (0.543)	-1.479 (0.821)
loc_{BB}	0.505 (0.032)	0.872 (0.061)	loc_{wB}	1.028 (0.092)	2.204 (0.113)
loc_{Brh}	-0.626 (0.141)	0.023 (0.15)	loc_{wrh}	-3.50 (0.392)	
loc_{Bt}			loc_{wt}	0.453 (0.141)	-0.419 (0.21)
loc_{BC}	0.046 (0.016)	-0.106 (0.03)	loc_{wC}	0.208 (0.045)	
n	635	631	n	635	607
ε_i	0.087	0.188	ε_i	0.238	0.381
Standard deviation for random effects			*Standard deviation for random effects*		
Estimate	0.179	0.27	Estimate	0.449	0.593
Lower	0.136	0.203	Lower	0.337	0.444
Upper	0.238	0.359	Upper	0.598	0.792

n=the sample number; ε_i = the residual variance.

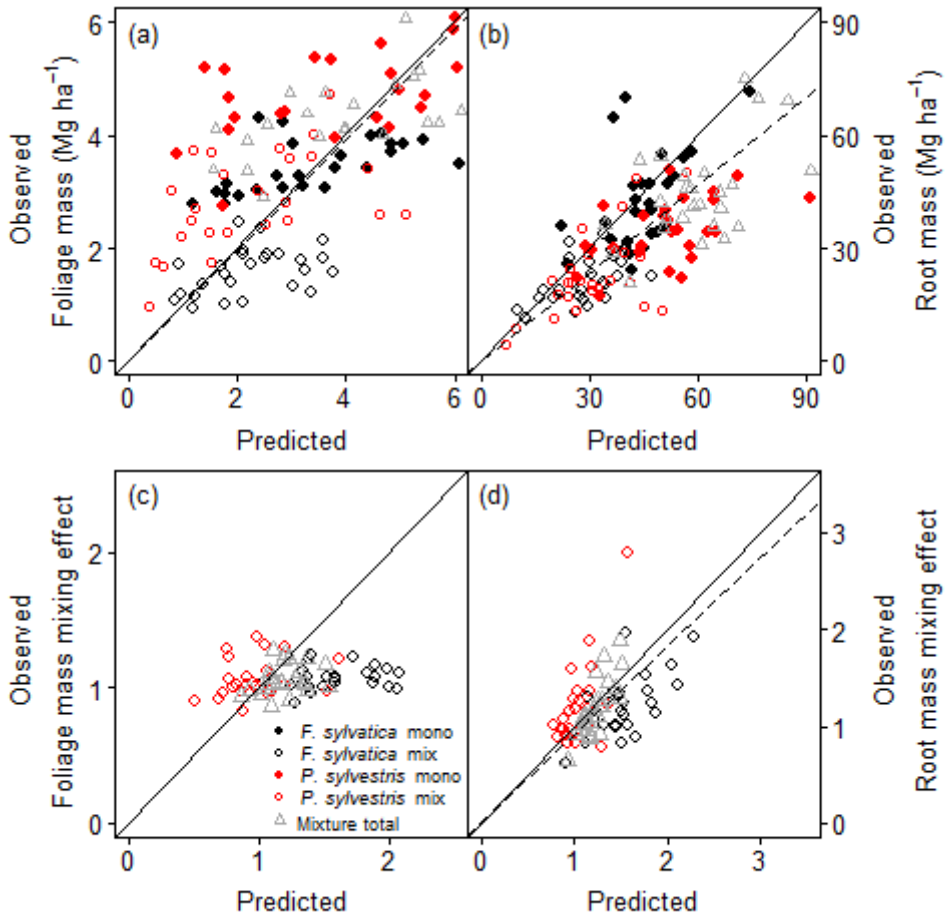

Figure B3. Comparison of observed and predicted foliage mass (W_F, a), root mass (W_R, b) and mixing effects on foliage mass (c) and root mass (d), all for the end of 2012. The solid lines are 1:1 lines and the dashed lines are lines fitted to the data that pass through the origin. For each species-treatment combination n=26.